

Effect of Sodium Citrate on Bitumen Droplets Coalescence

by

Xu Zhang

A thesis submitted in partial fulfillment of the requirements for the degree of

Master of Science

in

Chemical Engineering

Department of Chemical and Materials Engineering
University of Alberta

© Xu Zhang, 2021

Abstract

Hot water extraction technique has been applied to extract bitumen from oil sands for decades. With the challenge of low oil prices, achieving higher recovery and efficient production becomes more urgent. In recent years, the overall recovery and froth quality have been improved significantly when sodium citrate is used as a secondary process aid during oil sands extraction. The beneficial effects of sodium citrate on preventing slime coating, accelerating the liberation process, and enhancing bubble-bitumen attachment have been demonstrated in industry applications.

Bitumen droplet size is a key factor affecting the flotation recovery. A bigger bitumen droplet tends to attach to an air bubble easily and can be effectively floated. This research focuses on the fundamental effects of sodium citrate on bitumen droplet size and coalescence. In order to study the effects of sodium citrate on bitumen droplet size, experiments were performed using a high-speed camera, Focused beam reflectance measurement (FBRM) and Smart online particle analysis technology (SOPAT) with oil sands ore or bitumen samples under various water chemistries.

The beneficial effects of sodium citrate on bitumen droplet size and bitumen droplet coalescence have been observed when added with caustic into the oil sands system with process water. At an optimum dosage, bitumen droplet coalescence is increased when sodium citrate is added as a secondary processing aid in the bitumen emulsion system with either process water or synthetic process water. However, sodium citrate did not show any beneficial effect at high concentrations in either process water or synthetic process water. The use of sodium citrate alone did not show any beneficial effect on bitumen coalescence at the concentrations studied in deionized water at pH 8.5.

The fundamental mechanism affecting bitumen droplet interaction consists of the interplay of three major factors: slime coating, surface properties, and surface forces. The use of sodium citrate as secondary processing aid can prevent slime coating, which keeps the surface clean to enhance the droplet coalescence. Also, the electrical double layer (EDL) repulsion between bitumen droplet could be increased at a high concentration of sodium citrate, which prevents the droplet coalescence. In our recent studies, the use of sodium citrate might soften the interfacial film at bitumen-water interface, which may promote the bitumen droplet coalescence. Depending on the concentration of sodium citrate, the overall effect of sodium citrate on bitumen droplets coalescence depends on the balance of these three factors. The fundamental knowledge obtained in this research indicates that larger bitumen droplets can be induced at an optimum sodium citrate concentration, which in turn results in a higher flotation recovery.

Acknowledgements

First, I would like to thank my supervisor, Dr. Qingxia Liu, for giving me the valuable opportunity to be in the graduate program. Many thanks for making plans suitable for me, supporting me academically and giving me valuable advice.

I would like to thank Dr. Jun Long and Syncrude Inc. for providing the funding, materials and advice from an industry perspective.

I am thankful for the Natural Sciences and Engineering Research Council of Canada (NSERC)/Syncrude CRD project on the Secondary Process Aids in Bitumen Extraction from Oil Sands Ores to provide the financial support.

I am also grateful for all the help from the group members. Dr. James Grundy and Dr. Bo Liu have trained me on experiment equipment and given me so much inspiration and useful advice. Dr. Rogerio Manica and Dr. Yi Lu have helped me with theory and academic writings. Without your help, it would be much harder for me to discover the fundamental mechanism.

Last, I am grateful for all the emotional support from my loved ones, my parents and my partner.

Table of Contents

| | |
|--|-----------|
| 1. INTRODUCTION | 1 |
| 1.1. Background | 1 |
| 1.2. Research objective | 2 |
| 1.3. Thesis outline | 3 |
| 2. LITERATURE REVIEW | 5 |
| 2.1. Oil sands formation and water-based extraction process | 5 |
| 2.1.1. Liberation process | 7 |
| 2.1.2. Aeration process | 9 |
| 2.2. Bitumen composition, surface structure and electric properties | 10 |
| 2.3. Bitumen droplets coalescence process | 11 |
| 2.4. Factors affecting bitumen droplets coalescence | 13 |
| 2.4.1. Colloidal interaction between bitumen surfaces | 13 |
| 2.4.2. Effect of asphaltene on bitumen droplet coalescence | 17 |
| 2.4.3. Effect of clay on bitumen droplet coalescence | 19 |
| 2.5. Effects of sodium citrate on the oil sands extraction process | 21 |
| 3. BITUMEN DROPLET SIZE WITH SODIUM CITRATE IN OIL SANDS MIXING PROCESS | 23 |

| | |
|--|-----------|
| 3.1. Methodology | 23 |
| 3.1.1. Materials | 23 |
| 3.1.2. Experimental methods | 24 |
| 3.2. Results and discussion | 27 |
| 3.2.1. Bitumen droplet size with caustic | 27 |
| 3.2.2. Bitumen droplet size with caustic and sodium citrate | 31 |
| 3.2.3. Bitumen droplet size as a function of time | 34 |
| 3.2.4. Summary | 38 |
| | |
| 4. EFFECT OF SODIUM CITRATE ON BITUMEN DROPLET SIZE IN MODEL BITUMEN EMULSION SYSTEM WITH PROCESS WATER | 39 |
| | |
| 4.1. Methodology | 39 |
| 4.1.1. Materials | 39 |
| 4.1.2. Experiment method | 39 |
| | |
| 4.2. Results and discussion | 42 |
| 4.2.1. Effect of sodium citrate in process water (citrate pre-added) | 42 |
| 4.2.2. Effect of sodium citrate in process water (sodium citrate post-added) | 45 |
| 4.2.3. Effect of sodium citrate in fines-filtered process water | 47 |
| 4.2.4. Comparison between the cases with process water and discussion | 49 |
| | |
| 4.3. Effect of sodium citrate on clay on the bitumen droplet surface | 51 |
| | |
| 4.4. Summary | 52 |

| | |
|--|-----------|
| 5. EFFECT OF SODIUM CITRATE ON BITUMEN DROPLET SIZE IN MODEL BITUMEN EMULSION SYSTEM WITH SYNTHETIC WATER | 54 |
| 5.1. Methodology..... | 54 |
| 5.1.1. Materials | 54 |
| 5.1.2. Experiment set up..... | 54 |
| 5.2. Results | 59 |
| 5.2.1. Effect of single ions | 59 |
| 5.2.2. Effect of sodium citrate with divalent ions | 63 |
| 5.2.3. Effect of sodium citrate in synthetic process water..... | 65 |
| 5.3. Effect of sodium citrate on surface force between bitumen droplets | 70 |
| 5.4. Effect of sodium citrate on the surface property of bitumen droplets | 76 |
| 5.5. Summary..... | 76 |
| 6. CONCLUSIONS AND FUTURE WORKS | 78 |
| 6.1. Conclusions | 78 |
| 6.2. Future works | 80 |
| REFERENCES | 82 |

List of Tables

| | |
|--|----|
| Table 1. Concentration of caustic and sodium citrate for experiments..... | 23 |
| Table 2. Concentration of caustic and sodium citrate for experiments..... | 27 |
| Table 3. Bitumen droplet size and slurry pH as a function of caustic concentration. | 31 |
| Table 4. Synthetic process water recipe..... | 54 |
| Table 5. Salt concentration for FBRM experiment with multi-ions. | 58 |

List of Figures

| | |
|--|----|
| Figure 1. Schematic of oil sands extraction process. Reprinted from Ref. 9 with permission from John Wiley & Sons, Inc. | 6 |
| Figure 2. Relation of contact angle with interfacial tension at bitumen/sand interface..... | 8 |
| Figure 3. Relation of contact angle with interfacial tension at the bitumen/air interface..... | 9 |
| Figure 4. Oil droplet coalescence mechanism. | 11 |
| Figure 5. Mechanism of sodium citrate interaction with bitumen. | 22 |
| Figure 6. Experiment set up and procedure of bitumen droplet size measurement with oil sands and process water..... | 25 |
| Figure 7. Image analysis procedure for bitumen droplet size. (a) original image; (b) image after 8-bit grayscale transformation; (c) image after FFT bandpass and threshold adjustment. | 26 |
| Figure 8. Relation of cumulative volume fraction and bitumen droplet size in the presence of caustic alone. | 28 |
| Figure 9. D90 and D50 of bitumen size distribution at different caustic concentration..... | 29 |
| Figure 10. Colloidal interaction forces between bitumen surfaces as a function of separation distance. Reprinted from Ref. 10 with permission from Elsevier. | 30 |
| Figure 11. Cumulative bitumen droplet size volume-based fraction in the presence of caustic and sodium citrate..... | 32 |

| | |
|---|----|
| Figure 12. Histogram of bitumen droplet size distribution with caustic and sodium citrate..... | 33 |
| Figure 13. Cumulative volume-based bitumen droplet size distribution with 0.05 wt.% caustic at different mixing times. | 35 |
| Figure 14. Cumulative volume-based bitumen droplet size distribution with 0.05 wt.% caustic and 0.01 wt.% sodium citrate at different mixing times..... | 36 |
| Figure 15. Bitumen droplet size (D90, D50) as a function of time with 0.05 wt.% caustic alone and with 0.01 wt.% sodium citrate as SPA. | 37 |
| Figure 16. Use of SOPAT to detect bitumen droplets. Left: Original image. Right: Analyzed image. | 39 |
| Figure 17. Experiment set up for bitumen droplet size measurement with SOPAT. | 40 |
| Figure 18. Procedure of the set 1 experiment with process water. | 41 |
| Figure 19. Procedure of the set 2 experiment with process water. | 41 |
| Figure 20. Procedure of the set 3 experiment with process water. | 42 |
| Figure 21. Evolution of the bitumen droplet Sauter mean size in Na ₃ Cit pre-added process water..... | 44 |
| Figure 22. Bitumen emulsion images taken by SOPAT in Na ₃ Cit pre-added PW with 0-1 mM sodium citrate..... | 44 |
| Figure 23. Evolution of the bitumen droplet Sauter mean size in Na ₃ Cit post-added process water..... | 46 |
| Figure 24. Bitumen emulsion images taken by SOPAT in Na ₃ Cit post-added PW with 0-1 mM sodium citrate..... | 46 |

| | |
|---|----|
| Figure 25. Evolution of the bitumen droplet Sauter mean size in fines-filtered process water..... | 48 |
| Figure 26. Bitumen emulsion images taken by SOPAT in fines-filtered PW with 0-1 mM sodium citrate. | 48 |
| Figure 27. Bitumen droplet size difference between 0 minutes and the average of the last 5 minutes in PW, fines-filtered PW, and sodium citrate pre-added PW. | 50 |
| Figure 28. Possible mechanism of sodium citrate helping to prevent slime coating and promoting bitumen droplet coalescence..... | 52 |
| Figure 29. Experimental set up for bitumen droplet size measurement with FBRM. | 56 |
| Figure 30. Procedure of the set 1 experiment with synthetic water..... | 57 |
| Figure 31. Procedure of the set 2 experiment with synthetic water (adding calcium ions before emulsification). | 57 |
| Figure 32. Procedure of the set 3 experiment with synthetic water..... | 58 |
| Figure 33. Evolution of median bitumen droplet size in sodium citrate solution. | 60 |
| Figure 34. Size distribution chart with the addition of 1 mM sodium citrate. | 60 |
| Figure 35. Evolution of median bitumen droplets in calcium chloride solution. . | 61 |
| Figure 36. Size distribution chart with the addition of 1 mM calcium chloride.. | 62 |
| Figure 37. Median bitumen droplet size at 30 minutes as a function of sodium citrate concentration in the presence of calcium ions (adding calcium before making the emulsion, the droplet size among all cases is around $19 \pm 1 \mu\text{m}$ at 0 minute). | 64 |
| Figure 38. Evolution of Sauter mean bitumen droplet size in synthetic process water. | 66 |

| | |
|---|----|
| Figure 39. Bitumen emulsion images taken by SOPAT in SPW with 0-1 mM sodium citrate..... | 66 |
| Figure 40. Bitumen droplet size difference between 0 minutes and the average of the last 5 minutes in SPW, PW, fines-filtered PW and sodium citrate pre-added PW..... | 68 |
| Figure 41. Evolution of Sauter mean bitumen droplet size in synthetic process water at 45°C..... | 69 |
| Figure 42. Comparison of the evolution of Sauter mean bitumen droplet size in synthetic process water at room temperature and at 45°C..... | 70 |
| Figure 43. Zeta potential of bitumen droplets in pH 8.5 calcium solution as a function of sodium citrate concentration. | 71 |
| Figure 44. Zeta potential of bitumen droplets in synthetic process water as a function of sodium citrate concentration. | 72 |
| Figure 45. Colloidal interaction force between bitumen droplets in SPW with sodium citrate..... | 74 |

1. Introduction

1.1. Background

In 2019, Canada had 167.7 billion barrels' crude oil in proven reserves, and 162 billion mostly from Alberta's oil sands deposits.¹ Oil sands contain mineral solids, water and ultra-heavy oil, which is typically known as bitumen. Since bitumen is highly viscous and cannot flow at room temperature, the extraction from oil sands deposits is much harder than that from conventional oil reservoirs. One of the most common methods to produce bitumen from oil sands is by surface mining. During this process, oil sands ores are first mined from the open pit before being treated and transferred to the extraction plant. In order to extract the bitumen from oil sands, a water-based extraction process is applied, which uses hot water and “*caustics* (e.g., NaOH)” to liberate the bitumen from the gangue solids, and then recover the liberated bitumen by flotation.²

More recently, Syncrude Canada Ltd. has patented a new technology to further increase the bitumen recovery with limited expense. In general, a trace amount of sodium citrate is applied as a secondary process aid while NaOH is still used as the primary process aid. It was found that adding both chemicals together can improve not only the final bitumen recovery and froth quality, but also accelerate the bitumen production rate. Moreover, this technology has already been proven as very promising in a piloted-scale demonstration operated by Syncrude. However, there is still a lack of fundamental understanding of the mechanism of how sodium citrate improves various aspects of the extraction process.^{3,4}

The oil sands extraction process involves slurry preparation, hydrotransport, liberation, aeration, froth treatment, and tailings management.² During the liberation

process, bitumen detaches from its host surfaces and disperses into water.² Xiang et al. investigated the mechanism of sodium citrate in enhancing the bitumen liberation process.^{5,6} It was found that sodium citrate increases the repulsion between bitumen and sand particles, resulting in better liberation. Meanwhile, bitumen aeration is another important process because it determines the final recovery.^{7,8} Bitumen has almost the same density as water at the operating temperature used in hot water-based oil sands extraction.⁹ Therefore, bitumen needs to attach to air bubbles during aeration, which lowers the total density of bitumen significantly. Consequently, the as-formed bituminous froth can float to the top of the vessel for collection.²

Collision efficiency is one of the most critical parameters evaluating the flotation efficiency. Collision efficiency is proportional to the ratio of the size of bitumen droplet to the size of the air bubble, $E_C \propto (D_{bit}/D_{air})^n$. Therefore, a large bitumen droplet is more favourable for bitumen-bubble attachment and thereby, resulting in better recovery.⁹ However, increasing the bitumen droplet size is difficult due to the repulsive colloidal forces between bitumen surfaces, which are caused by bitumen surface properties and process water chemistry.¹⁰

1.2. Research objective

This research focuses on the effect of sodium citrate on bitumen droplets coalescence in aqueous solutions.

A large bitumen droplet is more favourable for better recovery. In order to increase the bitumen droplet size, coalescence between bitumen droplets needs to happen first. The

overall goal of this research is to understand if sodium citrate will affect the bitumen droplet size and how it affects the coalescence process.

The major research objectives of this M.Sc. thesis include:

- To investigate bitumen droplet coalescence in oil sands slurry mixing condition with sodium citrate;
- To investigate bitumen droplet coalescence in various model aqueous solution with sodium citrate;
- To understand the fundamental mechanism of how sodium citrate affects bitumen droplet coalescence based on colloidal interaction, interfacial property, and clay.

1.3. Thesis outline

Chapter 1:

- Introduces the research areas, statement of problems, objectives, and outline of this thesis.

- Discusses briefly the background on oil sands.

Chapter 2:

- Reviews the formation and composition of oil sands and the elementary steps in a water-based bitumen extraction process.

- Reviews the components, structures, and properties of bitumen droplets, and their roles in determining the bitumen droplet coalescence process.

Chapter 3:

- Presents the results of the bitumen droplet size test with sodium citrate in oil sands slurry mixing condition.

Chapter 4:

- Presents the results of the bitumen droplet size test with sodium citrate in the ideal model bitumen emulsion system with process water.

- Discusses the possible mechanism for bitumen droplet size change based on slime coating.

Chapter 5:

- Presents the results of the bitumen droplet size test with sodium citrate in the ideal model bitumen emulsion system with synthetic water.

- Discusses the possible mechanism for bitumen droplet size change based on interaction force and surface property.

Chapter 6:

- Concludes the key findings on the effect of sodium citrate on bitumen droplet size, and the mechanism behind it.

2. Literature review

2.1. Oil sands formation and water-based extraction process

Oil sands in Alberta are unique resources. Unlike conventional oil that can flow like a liquid in the reservoir, oil sands contain highly viscous bitumen attached to sand grains that is not able to flow in reservoir conditions.²

Two methods are commonly applied to recover bitumen from this unconventional oil resource: open-pit surface mining and in-situ thermal technologies. Open-pit mining followed by water flooding is generally used for the oil sands deposits less than 75 m beneath the ground. Trucks and shovels excavate the oil sands ore from the ground and the ore is transported to the extraction plant to separate the oil from sand and water.²

For the oil sands that are deeper than 75 m, steam-assisted gravity drainage (SAGD) technology is typically applied to extract bitumen through the in-situ operation. In this method, hot steam is injected into the reservoir to lower the viscosity of bitumen which allows bitumen to flow into the production well.²

Surface-mining followed by water-based extraction is the most mature and commercialized method nowadays, although SAGD is believed to be the future of the oil sands industry. Therefore, this study focuses on the water-based extraction method.

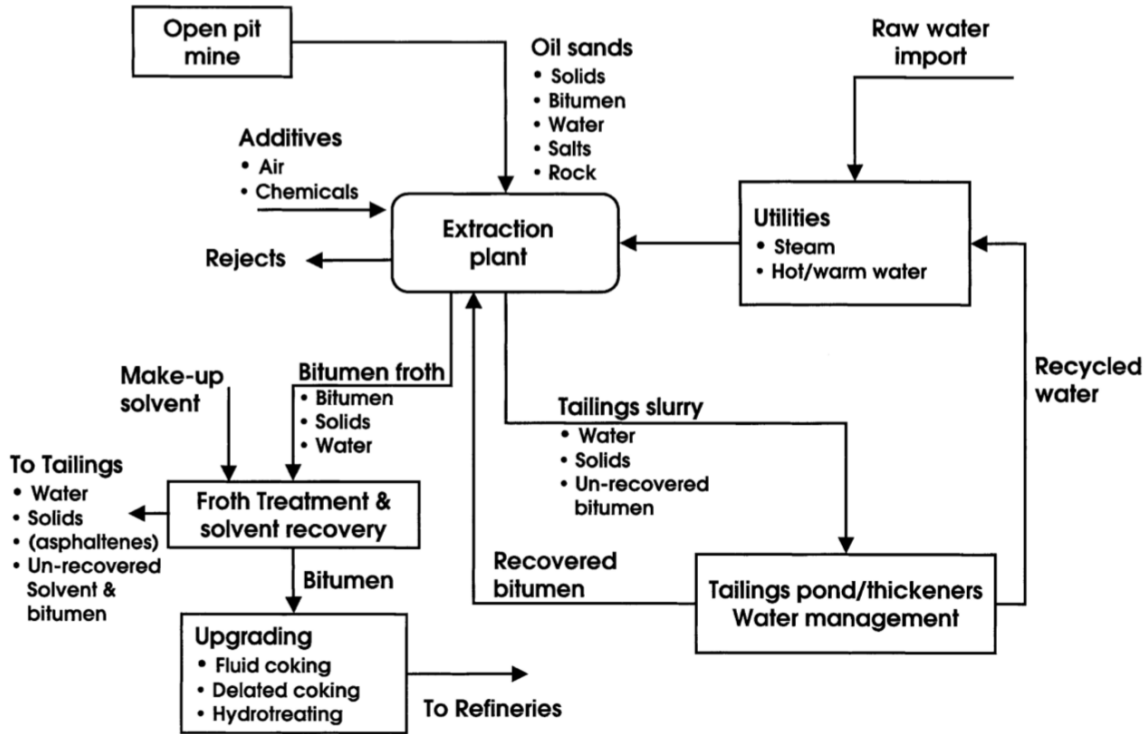


Figure 1. Schematic of oil sands extraction process. Reprinted from Ref. 9 with permission from John Wiley & Sons, Inc.

The hot water extraction process was first introduced by Dr. Clark.¹¹ The process is shown schematically in Figure 1.^{2,12} First, the mined oil sands ores are mixed with 80 °C hot water and sodium hydroxide to form an oil sands slurry, which is then transported in a hydrotransport pipeline before pumping into separation vessels. During the hydrotransport stage, the slurry conditioning happens, where the shear forces break the big lumps of ore into smaller ones layer by layer. Meanwhile, bitumen, sand and water also break apart from each other and form a dispersed solution.^{2,12} Bitumen liberation and aeration also happen in this dispersed solution during hydrotransport. Because of the added caustic, the pH alternation to 8.5 changed the interfacial tension of the sand and bitumen. Consequently, the contact angle on the sand grains decreases and the bitumen drop is then detached and

liberated from the sand surface. In the aqueous solution, the liberated bitumen droplets tend to coalesce. Eventually, air bubbles are applied and attached to bitumen droplets, lower the density of the bitumen and form a bituminous froth.^{2,12}

After hydrotransportation, the slurry is fed into the separation vessels, where the slurry separates into three layers by gravity: (1) The aerated bitumen on the top forms the primary froth, which is sent to froth treatment. (2) The sand settled at the bottom forms the tailing, which is sent to tailing treatment. (3) The bitumen, water, sand mixture in the middle part is middling, which is sent to a secondary separation vessel for further bitumen separation.^{2,9}

The froth collected from the hot water bitumen extraction process is not pure bitumen. In fact, it contains 60% bitumen, 30% water and 10% solid. This froth is sent to the froth treatment facility to recover purer bitumen. Organic solvent is used to separate the bitumen from the water and solids, and there are two major solvents commercially used: naphtha-based and paraffin-based solvent.^{2,9} In the end, tailing also needs to be treated before pumping into ponds and reclaim the land. Polymer and salt addition can accelerate solid aggregation and settling, however, tailing treatment is still a serious problem.^{2,9}

2.1.1. Liberation process

There are two sub-steps involved in the bitumen liberation. First, bitumen recedes on the sand surface, whereas the second step is bitumen detaching from the sand surface. Several factors can affect the whole liberation process, which can be explained by the Young's equation. (Figure 2)^{2,13,14}

$$\cos \theta = \frac{\gamma_{S/B} - \gamma_{W/S}}{\gamma_{W/B}} \quad (1)$$

where θ is the equilibrium contact angle and γ is the interfacial tension. S, B and W represent solid, bitumen and water, respectively. From Equation 1, in order to achieve better liberation, a smaller equilibrium contact angle is needed, which can result from a smaller $\gamma_{W/B}$ and/or $\gamma_{W/S}$. ($\gamma_{S/B}$ is almost constant at the operating condition)².

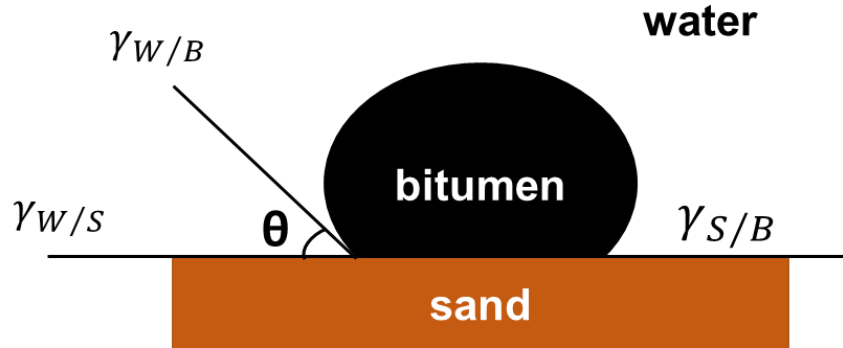


Figure 2. Relation of contact angle with interfacial tension at bitumen/sand interface.

Previous research showed that pH and water chemistry can affect the interfacial tension to control the contact angle, but it cannot change the contact angle to zero degrees. Therefore, the hydrodynamic force caused by agitation is essential to separate the bitumen from the sand grain.^{2,13,15}

With increasing pH, the contact angle decreases, which is beneficial to the liberation process.¹³ Higher pH results in a more negatively charged surface and the release of surface-active components from bitumen, which reduces the water-solid and bitumen-water interfacial tensions.¹³

With higher salt concentration, bitumen liberation is hindered. It could result from the compressed EDL double layer and reduced repulsive force.^{13,14,16,17} Moreover, in the presence of divalent cations, bitumen liberation could be further weakened. Calcium ions could absorb on the bitumen surface and reduce the repulsive force between bitumen and sand.¹⁵

2.1.2. Aeration process

The attachment of an air bubble onto a bitumen droplet is defined as bitumen aeration. After liberation, bitumen droplets are suspended in the slurry and need to attach to an air bubble in order to form a floc and lower the density. Eventually, bitumen floats and gets recovered.²

The aeration process is thermodynamic favourable. Therefore, as shown in Figure 3, air and bitumen should be attached. Based on the Gibbs free energy and Young's equation

$$\frac{\Delta G}{\Delta A} = \gamma_{A/W}(\cos \theta - 1) \quad (2)$$

it can be derived that the value of $\Delta G/\Delta A$ is always negative because $\cos \theta \leq 1$.²

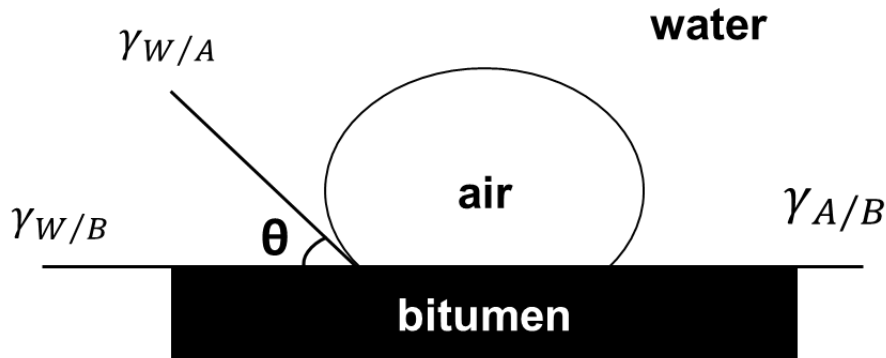


Figure 3. Relation of contact angle with interfacial tension at the bitumen/air interface.

However, before attachment between bitumen and bubble happens, a thin water film in between needs to be drained out first, and several factors can affect this process, such as pH, water chemistry, etc. In a pure system, smaller pH and higher divalent ions

concentration are favourable for aeration, because of the reduced repulsive force between bitumen and air bubble.^{2,18–20}

2.2. Bitumen composition, surface structure and electric properties

Bitumen is a natural mixture of hydrocarbons that contains about 15 - 21% saturated alkanes, 18 - 19% aromatics, 44 - 48% resins, and 14 - 20% asphaltenes.²¹ In addition, there are amphiphilic natural surfactants inside bitumen that can be extracted in alkaline aqueous solutions. Asphaltene is a paraffin-insoluble, colloidal-sized aggregate in bitumen. However, the molecular structures of asphaltenes are still under debate. Researchers have proposed several structures that contain aromatic rings with side carbon chains and molecular weights of 400 - 1500 Da.^{2,22}

The surface of bitumen in water is usually covered by asphaltene, natural surfactants, and clay minerals.² Bitumen surfaces are not smooth microscopically, but rather exhibit nanometer-sized bumps, which cause the interaction between bitumen droplets to behave differently from the smooth surface models, such as DLVO (Derjaguin–Landau–Verwey–Overbeek) theory^{23,24}. Wu et al.²⁵ used freeze-fracture scanning electron microscopy (FF-SEM) to observe the bitumen/water interface and found a rough bitumen surface. Protrusions from the surface were 50 - 100 nm in horizontal diameter, and the average vertical height was 38 nm.

The bitumen surface is usually negatively charged in water.² This phenomenon can be explained by the ionizable surface group concept.^{26,27} For bitumen, the negative surface charge results from the deprotonation of carboxylic acid ($\text{RCOOH} = \text{RCOO}^- + \text{H}^+$) and

amine ($\text{RNH}_3^+ = \text{RNH}_2 + \text{H}^+$) groups of natural surfactants adsorbed at the bitumen-water interface.²⁸

2.3. Bitumen droplets coalescence process

There are usually three steps for droplets to coalesce in an immiscible liquid medium, as illustrated in Figure 4.²⁹ First, the droplets approach each other until a thin liquid film is formed between them. Then, the film between the droplets starts to drain, resulting in reduced interfacial area. The thinning rate is mainly affected by capillary pressure and disjoining pressure. When surfactants are in the system, the thinning rate of the thin film can be slowed down by the Marangoni effect.³⁰ Studies have shown that polymers at the interface can also retard the thinning rate.³¹ After the thin film reaches a critical thickness, the film ruptures, and the droplets coalesce.

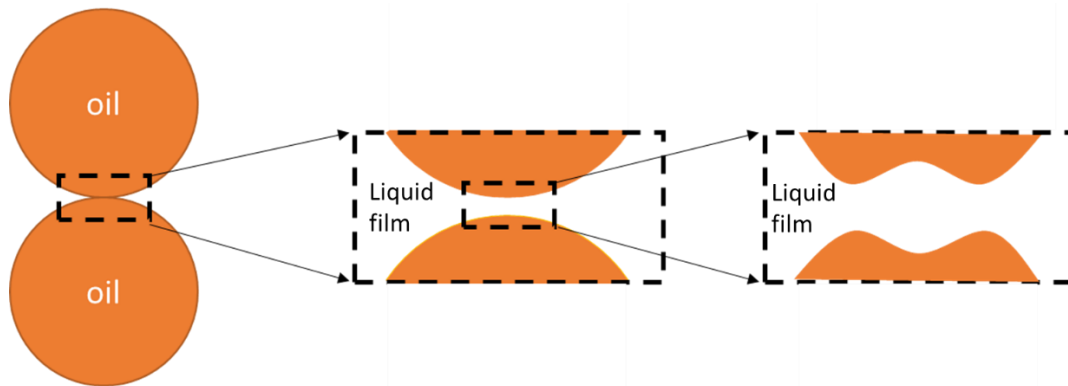


Figure 4. Oil droplet coalescence mechanism.

Oil droplets in an aqueous medium also follow this general coalescence mechanism (film drainage and film rupture). When two oil droplets approach each other, a thin liquid film forms between them with a minimum thickness at the centre. Due to the pressure on the film, a dimple structure, that means, an inversion of the film curvature, appears as film

drainage proceeds, and the minimum thickness is now at the rim.^{32,33} The dimple structure brings the surface of oil droplets closer which induces thin film rupture and the oil droplets coalesce.³⁴ Film drainage rate between oil droplets is mainly governed by the continuous phase viscosity, the film area, and the surfactant concentration.³² The film drainage rate is retarded by larger film areas and surfactant which creates an immobile interface. Film rupture is mainly affected by the interfacial properties, such as interfacial strength, interfacial charge, and steric hindrance. Interfacial viscoelasticity is a major kinetic barrier for droplets coalescence.³⁵

Bitumen coalescence mechanism has been studied using two main approaches:

(1) The focus is on the interaction forces between bitumen droplets. Wu et al. measured a much higher repulsive force than DLVO theory predicted when they assumed the bitumen surface was smooth.²⁵ Laroche measured more repulsive forces than the results predicted by Wu's disk protrusion model. The experimental result can be well explained by the steric hindrance model, which assumes a hair-like structure exists at the bitumen surface.³⁶ Aksoy found that bitumen droplets coalesce at a slow rate even though a strong repulsive force was present at separation distances smaller than 70 nm. The author concluded that coalescence occurred because of Van der Waals interaction and hydrophobic forces.³⁷

(2) The focus is on bitumen surface charge heterogeneity.³⁸⁻⁴⁰ Yeung et al. found no coalescence happened when two micrometre-sized bitumen droplets interacted directly in a fines-free solution.³⁸ However, when the two bitumen droplets interacted obliquely, coalescence occurred. In fines-free solutions, conventional DLVO theory can be applied to investigate the colloidal forces between two droplets. The calculated DLVO theory showed that there should be a strong repulsion between the two surfaces, which should prevent

coalescence when two bitumen droplets hit each other. However, since the bitumen surface is heterogeneous,² it is believed that shear may be able to remove heterogeneity or otherwise change the surface structure of bitumen. In Pickering emulsions, the process of thin film drainage sweeps out the particles at the interface, allowing the droplets to form a bridge before coalescence.⁴¹ Yeung et al.³⁸ believed that a steric layer could be torn off by the shearing motions of bitumen droplets so that the total repulsion could be lowered. Once the structure was broken, a bridge between bitumen droplets was formed across the solution, which then led to coalescence. The coalescence rate was determined by the deformation degree and droplet size.⁴⁰ Similarly, Whitby et al. also found that the particle network at the oil droplets interface could be broken and the oil droplets could coalesce with shear in a model system (bromohexadecane-in-water Pickering emulsions).⁴²

2.4. Factors affecting bitumen droplets coalescence

Colloidal interaction, asphaltene and clay are known to be detrimental to the bitumen droplet coalescence process.²

2.4.1. Colloidal interaction between bitumen surfaces

DLVO theory assumes the total interaction energy in a colloidal system is the sum of van der Waals (VDW) energy and electrical double layer (EDL) energy. When the discrepancy between experiment and theory occurred, researchers proposed non-DLVO interactions. The non-DLVO or extended-DLVO terms include steric repulsion, polymer bridging, hydration effects, and hydrophobic interactions.² Steric repulsion is caused by large, adsorbed molecules on the colloidal surfaces. The adsorbed layer, often polymers,

acts as a physical barrier to keep the particles apart. Since the attractive VDW force decays with the distance between particles, the weak attractive forces are not enough to let particle surfaces touch if the distance of steric repulsion is large enough.² Researchers have found that asphaltene could act like a polymer that creates steric hindrance through its aliphatic side chains.⁴³⁻⁴⁵

Water molecules form hydrogen bond networks and molecular clusters in bulk solution, however, water molecules cannot form hydrogen bonds with a hydrophobic surface nor form clusters between two close hydrophobic surfaces. Therefore, an attractive hydrophobic force tends to form between two close hydrophobic surfaces.²

Yoon et al. first explored the use of atomic force microscopy (AFM) to measure colloidal forces between bitumen surfaces. It was found that the bitumen-bitumen interaction was repulsive, and the asphaltene tails were present on the bitumen surface.^{46,47} The colloidal forces measured by AFM between bitumen surfaces were repulsive with a “jump in” at close separation. Experimental data did not fit the traditional DLVO theory below 18 nm separation distance. It was observed that the force measured was more attractive than the force DLVO theory predicted for these close separations. Because the bitumen surface is hydrophobic, the extended DLVO theory that considered hydrophobic and steric forces was invoked to explain the measured forces.¹⁰

The best-fit power-law constant for hydrophobic forces (100×10^{-21} J) was much larger than the Hamaker constant between bitumen surfaces in water (2.8×10^{-21} J), which means that the hydrophobic force was much stronger than van der Waals forces.¹⁰ A strong repulsive steric force only affected the interaction at a short distance (below 6 nm). After the jump in, the bitumen surfaces can deform and steric hindrance can happen because of

the asphaltene like macromolecules on the surface.¹⁰ Therefore, the dominant long-range forces between bitumen surfaces should be attributed to the EDL and hydrophobic forces, while steric force only dominates the short-range interaction.¹⁰

2.4.1.1. Effect of pH on colloidal interaction

Interaction forces between bitumen surfaces become more repulsive with increasing pH. Such trends can be explained by extended DLVO theory, where the fitted hydrophobic force constant decreases with the increasing pH, implying that the pH of the solution can affect the strength of the hydrophobic force. Additionally, measurements of the contact angle of air bubbles on bitumen surfaces also showed that the contact angle decreased with increasing pH, which illustrates that the bitumen surface becomes less hydrophobic at higher pH values.¹⁰

As discussed previously, surfactants are released from bitumen in alkaline conditions, which results in the variation of hydrophobic adhesion force. At lower pH, amine groups (RNH_3^+) are formed by the protonated cationic surfactants on the bitumen surface. These surface-anchored, positively charged groups can interact with aqueous OH^- or anionic surfactants (RCOO^- and ROSO_3^-) on the bitumen surface, so that a strong adhesion occurs between the two surfaces.¹⁰

At high pH, most of the surfactants released from bitumen into the slurry during the extraction process were found to be anionic surfactants of carboxylates and sulphates/sulphonates.⁴⁸ At higher pH, amine ions (RNH_3^+) deprotonate and reduce the electrostatic attraction to carboxylate groups, resulting in a weak adhesion force between bitumen droplets.¹⁰

Therefore, a lower pH is favourable for bitumen coalescence during the aeration process; however, the operational pH in the oil sands industry is around 8 to 9 to ensure overall higher recovery.²

2.4.1.2. Effect of salinity on colloidal interaction

The overall long-range interaction force decreases with increasing KCl dosage. A high concentration of salt can compress the EDL, which results in lower EDL forces. Meanwhile, at higher salt concentrations, more hydrophilic electrolyte ions can adsorb on the bitumen surface, which could further lower the hydrophobic effect slightly.¹⁰ Overall, the high concentration of electrolyte has a much stronger impact on EDL forces than hydrophobic forces, which makes the overall total force less repulsive. Therefore, the coalescence of bitumen droplets is more likely to happen at high salt concentrations. However, coalesced droplets are not as stable due to lower hydrophobic adhesion, and larger droplets have the potential to break up into smaller droplets by hydrodynamic forces.¹⁰

The results show consistency with Wu's finding that high salinity may compress the height of the "bump" on the bitumen and result in a higher chance of coalescence.²⁵ Wu et al. simplified the surface structure of bitumen and combined all the "bumps" on the surface into one uniform bump and used DLVO theory to calculate the interaction forces between the bitumen surfaces. The results showed a more repulsive force between the bitumen surfaces with the presence of the "bump". If there was a "bump" on the surface, the probability of coalescence upon collision was higher with a smaller bump. The same

study also found the bump height was compressed with high salinity, and a “bump” cannot prevent bitumen coalescence at electrolyte concentrations above 1 mM KCl.²⁵

2.4.1.3. Effect of divalent ions on colloidal interaction

Calcium ions affect both EDL force and hydrophobic forces by compressing the EDL and changing bitumen surface characteristics.¹⁰ Consequently, the hydrophobic force becomes weaker with the presence of calcium ions in the solution, because calcium ions can attach to the deprotonated carboxylic groups on the bitumen surface. This interaction between calcium ions and carboxylic groups can also lower the charge density on the bitumen surface, which reduces the EDL repulsion.¹⁰ Gan and Liu showed that a higher dosage of divalent ions caused a reduction in the absolute value of the zeta potential, which agreed with the force measurements.⁴⁹ Lin used a micropipette technique to measure the coalescence probability between two bitumen droplets and found that the coalescence probability increased with higher calcium ions concentration.³⁹ Therefore, divalent cations are considered to cause a reduced repulsive energy barrier and weaker attraction forces, enabling easier bitumen coalescence.¹⁰

2.4.2. Effect of asphaltene on bitumen droplet coalescence

Asphaltene is the fraction of bitumen, which can precipitate in paraffinic solvents but not in naphthenic solvents.⁵⁰ The molecular structure of asphaltene is still unknown, but researchers have used methods like X-ray scattering to propose some models. Among all the models, the archipelago model and the island model are the most recognized.^{51,52}

The archipelago model describes asphaltene molecules as polycyclic aromatic hydrocarbon groups connected by aliphatic chains, while the island model states that asphaltenes are one polycyclic aromatic hydrocarbon group consisting the intramolecularly connected aromatic rings with aliphatic side chains.⁵¹

Asphaltene molecules can further interact with each other and form complex structures. The net interaction is mainly contributed by attractive London dispersion, π - π stacking, and repulsive steric forces. This net interaction leads to asphaltene aggregation in the solvent. Asphaltene molecules tend to form nanoaggregates with an aggregation number of 6, which is the critical nanoaggregate concentration of asphaltene. The nanoaggregates then form clusters, which can be formed by nanoaggregates with an aggregation number of 8.⁵³⁻⁵⁵

Asphaltene is an interfacially-active component of bitumen. It can adsorb at the oil-water interface and form a stable film to hinder droplets coalescence.⁵⁶⁻⁵⁸ Several researchers have studied the water-oil-water thin film drainage process by monitoring the film lifetime, which represents the stability of the film.^{59,60} Asphaltene can stabilize the film at a final thickness of 40-90 nm at 0.5-2 g/L asphaltene concentration, while maltene can only maintain an 11 nm film at much higher added concentrations of 10-50 g/L. The large film stabilized by asphaltene may result from the ageing effect of asphaltene in which aggregates are formed, making complicated 3D structures at the oil-water interfaces.⁶¹

Salinity, pH and divalent ions can also affect the interaction between asphaltene layers. Liu et al.⁶² found that the interaction is more repulsive under high pH, low salinity and low divalent ions concentrations. Therefore, asphaltene may play an important role in the thin film drainage between bitumen droplets. Using AFM, Shi et al. studied the interaction between model oil droplets containing asphaltene and found that asphaltene

prevented the water film from draining.⁶³ However, no research has been performed to investigate the water film drainage between two bitumen droplets.

2.4.3. Effect of clay on bitumen droplet coalescence

In the oil sands industry, fines refer to mineral solids smaller than 44 microns. They are detrimental to many operations in the oil sands industry. Fines mainly involve various clays. Kaolinite accounts for 69% of clay in oil sands, while illite accounts for 28%. They are the biggest fractions in the clay. On the other hand, montmorillonite only accounts for 0.3% of the clay, but it is the most troublesome due to its swelling behaviour.²

Clay minerals are composed of two basic layers: silicon-oxygen tetrahedron sheet (T) and aluminum-oxygen-hydroxyl octahedron sheet (O). Kaolinite is a two layers clay that has a T-O structure, while illite and montmorillonite are 3 layers clays that have T-O-T structures. Due to the T-O structure, kaolinite has a stable structure and is classified as non-swelling clay. Isomorphic substitution at T-sheet makes the kaolinite base plane negatively charged. Illite is also a no swell clay, but the base surface is more negatively charged due to its looser structure. On the contrary, montmorillonite is a swelling clay because interlayer binding between the building blocks is weak.²

Clay can attach to bitumen by colloidal interactions, and the slime coating effect happens when the bitumen droplet is covered by a layer of fine clays. Slime coating often results in lower bitumen recovery.² Slime coating not only creates a steric hindrance barrier for bitumen-air attachment during flotation but also increases the difficulties of froth treatment.^{8,64,65} Calcium ions are believed to be the main reason for slime coating. It can link the bitumen surface to the clay surface and induce attachment. With zeta potential

distribution and QCM-D technology, researchers have further proved that not all clay particles can cause severe slime coating. With montmorillonite, calcium ions can cause severe slime coating. However, the attachment is not obvious with kaolinite and illite.^{8,64-67} During the bitumen coalescence process, it was also found that the existence of clay minerals has a negative impact because of the steric barrier clay created.¹⁰

Clay particles are naturally hydrophilic, but in oil sands slurry, they can be contaminated and become hydrophobic. Hannisdal et al. tested which bitumen components could be absorbed on mineral particles and make them hydrophobic.⁶⁸ QCM-D results suggest that both resin and asphaltene can adsorb at the silica surface in the form of multilayer or aggregate. Asphaltenes are irreversibly adsorbed as a rigid film. However, the amount of adsorbed resin is significantly smaller than that of asphaltene. The adsorption process can be divided into two phases. First, significant adsorption of bitumen fractions happens on hydrophilic particles, causing the wettability alternation and surface charge changes. Secondly, once the particle becomes hydrophobic, it will only adsorb smaller amounts of asphaltenes and resins, which leads to minor wettability changes.

Li observed that the bitumen droplet size decreasing in emulsion after adding mineral particles, and hydrophobic illite particles will further decrease the bitumen droplet size.⁶⁹ Nallamilli and Basavaraj found that surfactant hydrophobized kaolinite can help the formation of O/W emulsion, and increase the emulsion stability from two separated phases.⁷⁰ Whitby et al. showed that in a dodecane-in-water emulsion, hydrophobized Titania particles would attach to the interface and form Pickering emulsion.⁷¹ If hydrophobized Titania particles were mixed with silica, silica particles were entrapped in the Titania particle layer, and prevented Titania particles from attaching at the interface

and lowering the emulsion stability. Fu et al. found that the organic matter in ore can coat the clay particles. Those particles can attach to bitumen, preventing bitumen droplet size from increasing.⁷² Chen and Li used nano-SiO₂ to form bitumen Pickering emulsion and showed good stability.^{73,74}

Previous research also showed that clay can hinder bitumen droplet coalescence and hydrophobic clay can stabilize the emulsion better. Li believed hydrophobic force causes clay attachment on bitumen.⁶⁹

2.5. Effects of sodium citrate on the oil sands extraction process

Citrate can chelate calcium ions in an aqueous solution. In the food industry, citrate has been used to remove the heavy metals in the processing of cooking oils.⁷⁵ Xiang et al. showed that adding sodium citrate alone in bitumen emulsions increased the absolute value of the bitumen zeta potential.^{5,6} Stronger EDL repulsion between bitumen and clay induced by sodium citrate led to better liberation recovery. Bai et al. found that the more negatively charged bitumen surface caused by sodium citrate could reduce bubble-bitumen attachment probability at a given ionic strength.⁷⁶ However, sodium citrate could have little negative effect on bubble-bitumen attachment at high salinity, when Ca²⁺ coexisted with sodium citrate.

The mechanism for sodium citrate making the bitumen surface more negatively charged is most likely the chelation effect with Ca²⁺ ions, which removes the surface-bound metal ions, or caused by the deagglomeration and dispersion of surface-active compounds (Figure 5).⁴⁹

Compared to the zeta potential of bitumen with divalent ions, the presence of citrate increased the absolute value of the zeta potential of bitumen droplets by around 30 mV, which means that EDL repulsion in the divalent cation/citrate system is stronger than with only divalent ions.⁴⁹

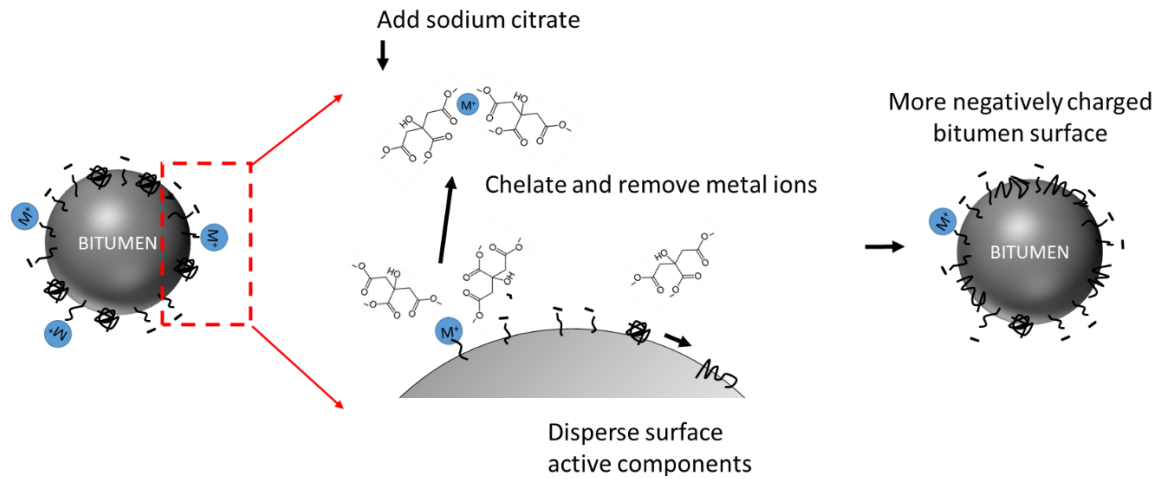


Figure 5. Mechanism of sodium citrate interaction with bitumen.

Zhang studied the effect of sodium citrate on slime coating and found that sodium citrate could prevent slime coating if added before slime coating happened. However, if the slime coating had already happened, sodium citrate did not have the ability to remove the slime coating.⁷⁷ Sodium citrate could also prevent slime coating by reducing the bitumen-clay attachment, because of the more negatively charged bitumen and clay surface and the reduced bridging effect caused by calcium ions. This effect is more significant on slime coating induced by montmorillonite-bitumen attachment.⁷⁷

3. Bitumen droplet size with sodium citrate in oil sands mixing process

3.1. Methodology

3.1.1. Materials

Oil sands and process water samples were provided by Canada Syncrude Ltd. Oil sands sample contained 8.3 wt.% of bitumen, which can be considered as poor-quality ores. Oil sands samples also contained 40 wt.% of fine particles on the basis of their solid content. The process water has a pH of 8.5 ± 0.1 .

The sodium hydroxide (NaOH) and sodium citrate (Na₃Cit) used in this study were analytical grade and were purchased from Fisher Scientific. The dosage for each experiment setup is listed in Table 1.

Table 1. Concentration of caustic and sodium citrate for experiments.

| Set | NaOH concentration (wt.%) | NaOH concentration (mM) | Na ₃ Cit concentration (wt.%) | Na ₃ Cit concentration (mM) |
|-----|---------------------------|-------------------------|--|--|
| 1 | 0 | 0 | 0 | 0 |
| 2 | 0.00625 | 1.56 | 0 | 0 |
| 3 | 0.0125 | 3.125 | 0 | 0 |
| 4 | 0.025 | 6.25 | 0 | 0 |
| 5 | 0.05 | 12.5 | 0 | 0 |
| 6 | 0.075 | 18.75 | 0 | 0 |
| 7 | 0 | 0 | 0.01 | 0.34 |
| 8 | 0.05 | 12.5 | 0.005 | 0.17 |
| 9 | 0.05 | 12.5 | 0.01 | 0.34 |

3.1.2. Experimental methods

This study has two experimental setups based on time: (1) investigate the bitumen size number after 30-minute of mixing, and (2) investigate the evolution of bitumen size over the period of 0-30 minutes.

3.1.2.1. Bitumen droplet size number at 30 minutes

The measurements of bitumen droplet size can be divided into 3 parts: mixing, image acquisition, and image analysis, as illustrated in Figure 6.

During the mixing process, 20 g of bitumen and 20 ml of process water were added together with/without caustic and/or sodium citrate, and then the mixture was heated to 45°C. The temperature was kept constant at 45°C during mixing. A stir bar inside the slurry was stirred with 1000 RPM mixing speed for 30 minutes. 1 ml of mixing slurry sample was collected by a pipette at 30 minutes and transferred into a glass cubic container, which contained 100 ml DI water inside.

The glass cubic container was surrounded by LED lights, a high-speed camera (Basler acA2000-165uc), of which the setup was designed to capture images of bitumen droplets in the slurry. Once the slurry was transferred to the container, a glass stir bar inside the container was used to stir at 200 RPM speed, and the camera captured pictures at 2 frames per second with 300 μ s exposure time for 1 minute.

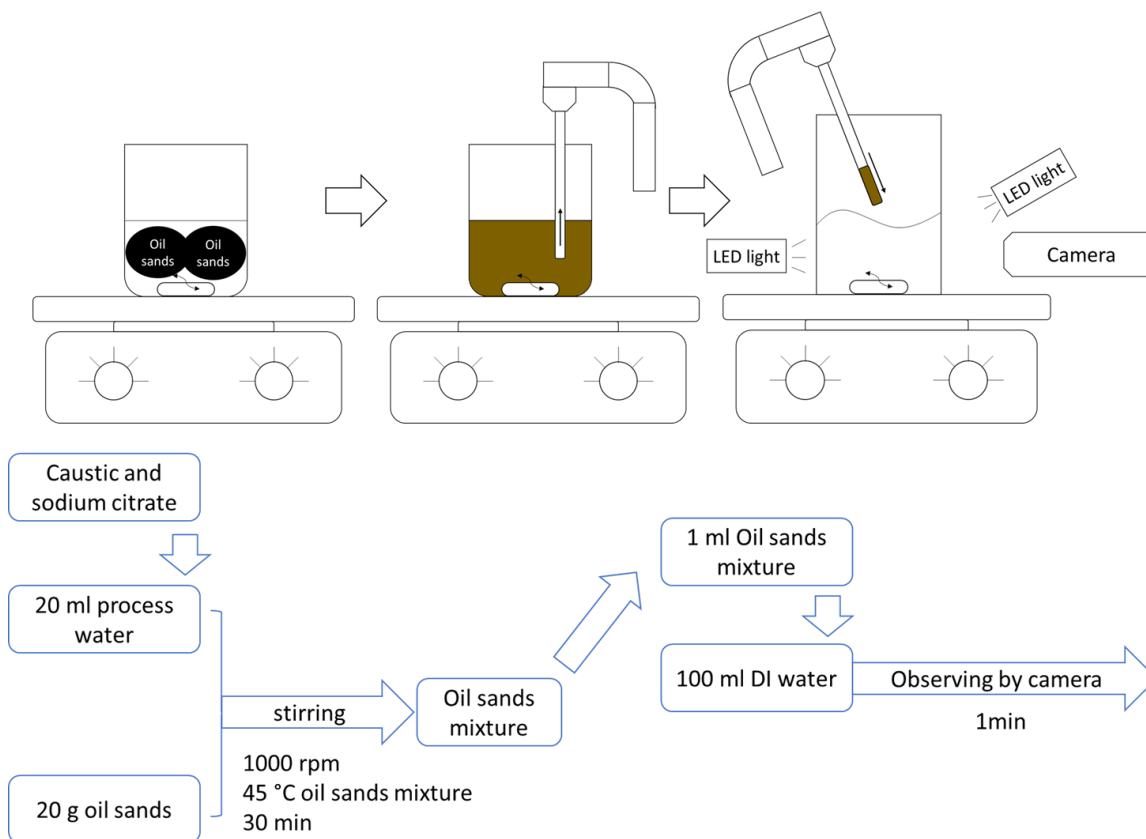


Figure 6. Experiment set up and procedure of bitumen droplet size measurement with oil sands and process water.

Image analysis was done with ImageJ software. The image was converted to an 8-bit greyscale before going through the Fast Fourier transform (FFT) bandpass filter (filter_large=40, filter_small=10, suppress=None, tolerance=5, autoscale saturate) to smooth the boundary and increase contrast. A threshold (0, 79) was then applied to the image to eliminate elements except for black bitumen droplets. The particle analysis tool was then used to measure the area of each particle and calculate the diameter of the bitumen droplets. 120 pictures were processed for each caustic and/or sodium citrate concentration to create size distribution curves.

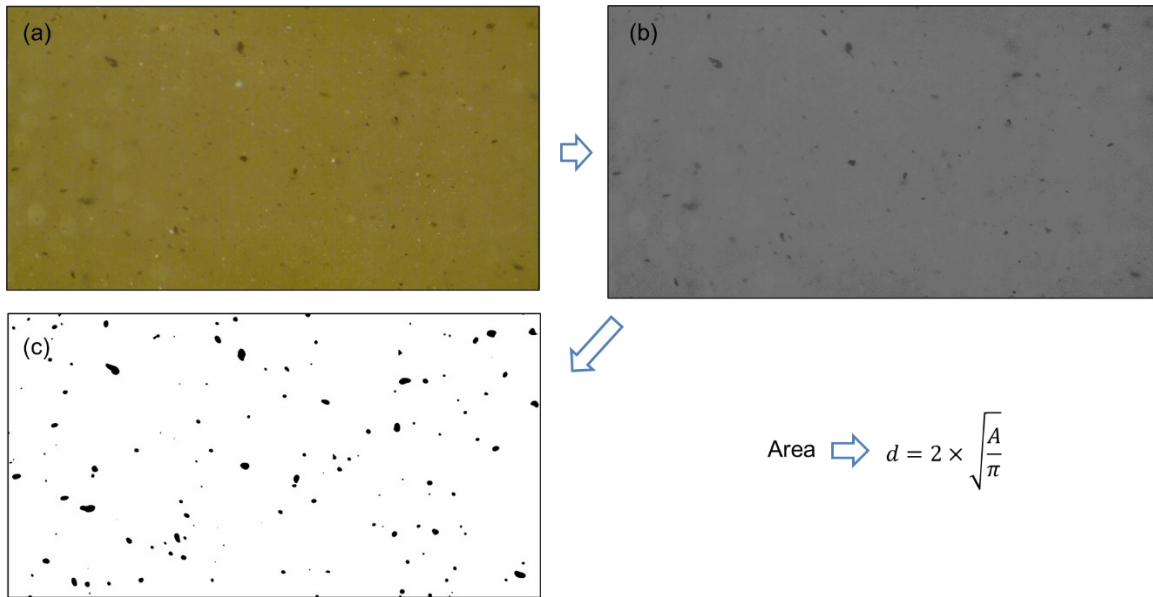


Figure 7. Image analysis procedure for bitumen droplet size. (a) original image; (b) image after 8-bit grayscale transformation; (c) image after FFT bandpass and threshold adjustment.

3.1.2.2. Bitumen size evolution over 0-30 minutes

The experimental setups for the measurements of the bitumen size evolution were the same as the bitumen droplet size measurement as described in Section 3.1.2.1 (including mixing, image acquisition and image analysis technique), except that the sample acquisition during the evolution tests was conducted at a time series of interest during the mixing duration. In this study, bitumen slurry samples were picked and transferred to take pictures at 5, 10, 20 and 30 minutes from starting mixing. The concentration of the chemical used in this experiment is listed in Table 2.

Table 2. Concentration of caustic and sodium citrate for experiments.

| Set | NaOH concentration (wt.%) | NaOH concentration (mM) | Na ₃ Cit concentration (wt.%) | Na ₃ Cit concentration (mM) |
|-----|---------------------------|-------------------------|--|--|
| 1 | 0.05 | 12.5 | 0 | 0 |
| 2 | 0.05 | 12.5 | 0.01 | 0.34 |

3.2. Results and discussion

3.2.1. Bitumen droplet size with caustic

Based on an oil sands extraction patent⁴, caustic added inside the slurry has a correlation with fines content in oil sands in order to achieve the best liberation. The correlation is given as

$$y = 0.024x - 0.0088 \quad (3)$$

where y is the caustic dosage (wt.% of oil sands ore) and x is the ratio of the fines content (%) over bitumen content (%). From Eq. 3, the best dosage of caustic is 0.05 wt.% for recovery of the used sample.

In order to have a full picture of how caustic addition affects bitumen droplet size, experiments were conducted with 0 wt.%, 0.00625 wt.%, 0.0125 wt.%, 0.025 wt.%, 0.05 wt.% and 0.075 wt.% of caustic dosage.

As can be seen from Figure 8, with the addition of caustic, the cumulative volume fraction line shifted left, which means the bitumen droplets tended to be smaller with increasing caustic dosage. In general, more caustic addition caused the bitumen size distribution to move towards the smaller size region.

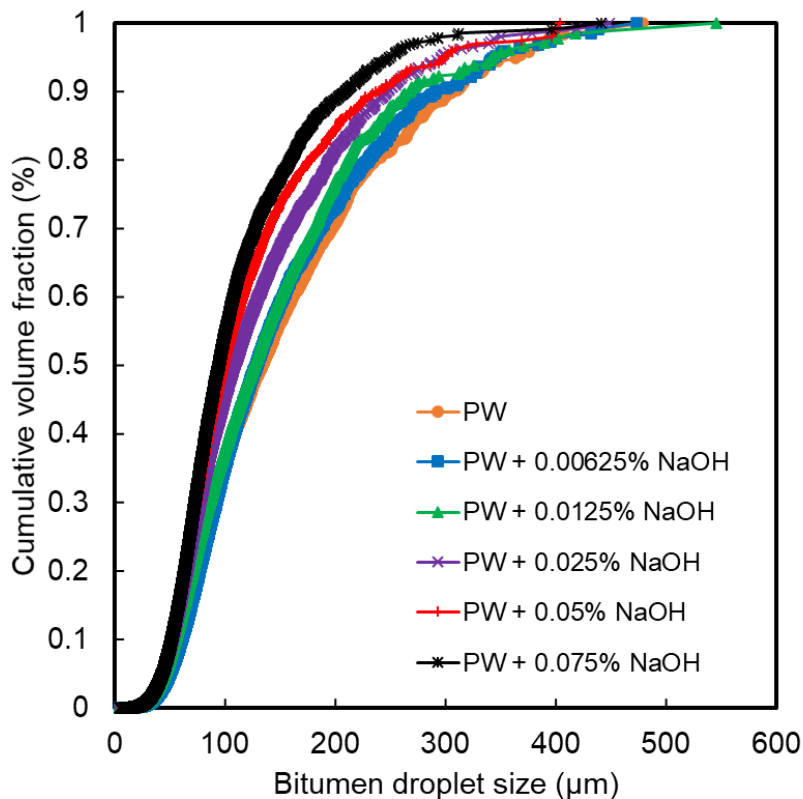


Figure 8. Relation of cumulative volume fraction and bitumen droplet size in the presence of caustic alone.

Bitumen droplet size change was evaluated by their D90 and D50 values. D90 and D50 represent the size at which 90% and 50% of particles are smaller than that size, respectively. Therefore, D90 shows the size bigger bitumen droplets can get, and D50 shows the median bitumen droplet size.

From Figure 9 and Table 3, it can be observed that a small amount of caustic (0.00625 wt.%) did not affect bitumen size distribution significantly. However, at 0.05 wt.% of caustic addition, which is the best dosage for bitumen recovery, caustic significantly reduced the D90 value of bitumen droplets from around 305 μm to 235 μm . Meanwhile, the D50 value also reduced slightly from around 126 μm to 103.6 μm . With 0.05 wt.%

caustic, the reduced D90 and D50 values mean that there was a significant decrease in the general bitumen droplet size, especially in the big droplet region.

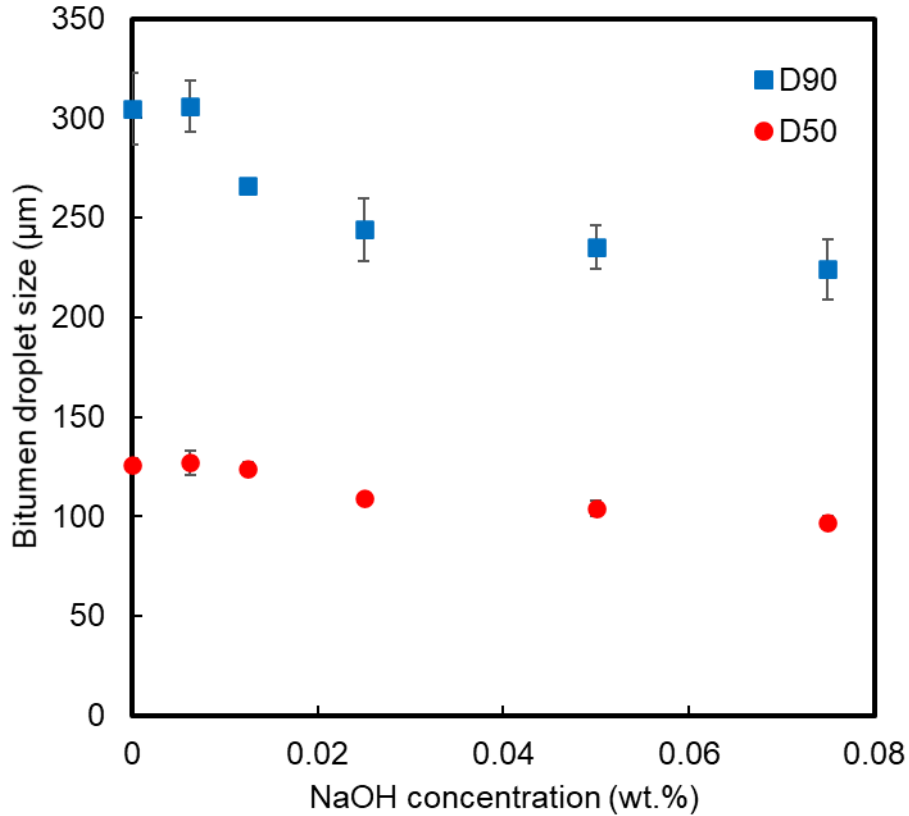


Figure 9. D90 and D50 of bitumen size distribution at different caustic concentration.

As mentioned in Chapter 2, a higher pH leads to better liberation, but worse aeration. With more caustic added in the slurry, the pH jumped from 8.5 to 10.4 at the experimental condition (Table 3). At $\text{pH} > 10$, the electrostatic repulsion between bitumen droplets is much stronger than the adhesion force, which prevents bitumen coalescence.¹⁰ Liu et al. studied the interaction forces between bitumen surfaces and found that there is no jump in phenomenon on the force curve at $\text{pH} 10.5$. This means that the bitumen surfaces did not attach to each other at $\text{pH} 10.5$, whereas at $\text{pH} 8.2$, the adhesion force was still stronger

than the repulsive force, which facilitated attachment (Figure 10).¹⁰ Therefore, adding caustic in the slurry, which results in higher pH, is not favourable for bitumen droplets coalescence. The best caustic dosage 0.05 wt.% is not favourable for bitumen droplet size increase.

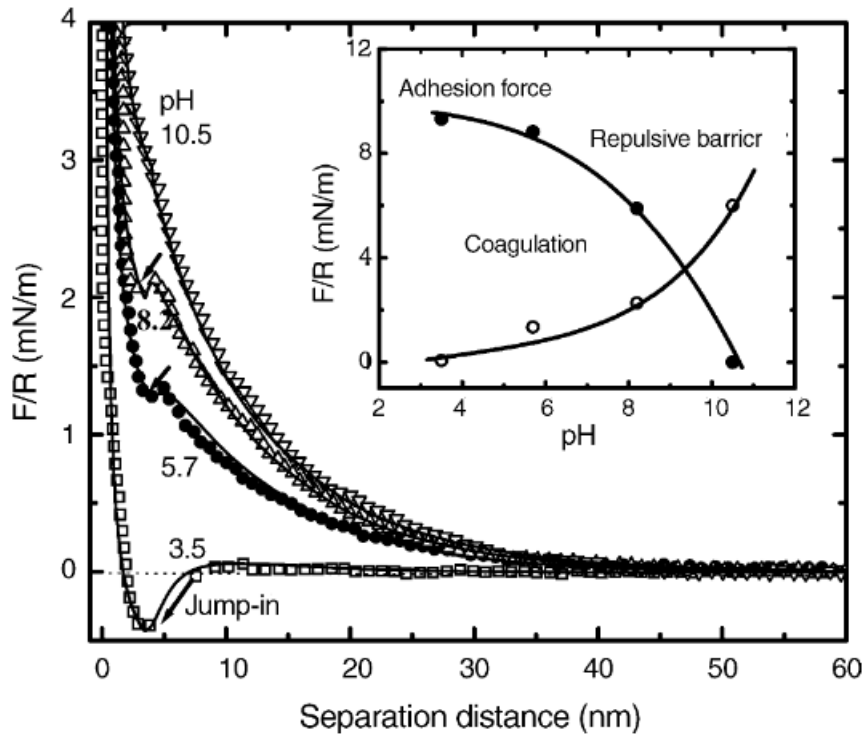


Figure 10. Colloidal interaction forces between bitumen surfaces as a function of separation distance. Reprinted from Ref. 10 with permission from Elsevier.

Table 3. Bitumen droplet size and slurry pH as a function of caustic concentration.

| | | | | | | |
|------------------------------|---------------|---------------|---------------|----------------|----------------|----------------|
| NaOH concentration (wt.%) | 0 | 0.00625 | 0.0125 | 0.025 | 0.05 | 0.075 |
| NaOH concentration (mM) | 0 | 1.56 | 3.125 | 6.25 | 12.5 | 18.75 |
| D90 (μm) | 305 \pm 18 | 306 \pm 13 | 266 \pm 2 | 244 \pm 16 | 235 \pm 11 | 224 \pm 15 |
| D50 (μm) | 126 \pm 3 | 127 \pm 6 | 124 \pm 3 | 109 \pm 2 | 104 \pm 4 | 97 \pm 3 |
| pH (before adding oil sands) | 8.5 \pm 0.1 | 9.2 \pm 0.1 | 9.7 \pm 0.1 | 10.1 \pm 0.1 | 11.2 \pm 0.1 | 11.9 \pm 0.1 |
| pH (after adding oil sands) | 8.3 \pm 0.1 | 8.8 \pm 0.1 | 9.0 \pm 0.1 | 9.4 \pm 0.1 | 10.0 \pm 0.1 | 10.4 \pm 0.1 |

3.2.2. Bitumen droplet size with caustic and sodium citrate

Sodium citrate has been proven to increase bitumen recovery as a secondary process aid (SPA). As a SPA, the effect on liberation has been demonstrated to be promising, but it also has a mixed effect on bitumen bubble interaction.^{4,5,76} The effect of SPA on the bitumen-bitumen interaction, especially on the bitumen droplet size, is discussed in this section.

As shown in Figure 11, adding 0.01 wt.% sodium citrate alone has a similar effect to adding 0.05 wt.% caustic alone, both of them are not beneficial for bitumen droplet size increase. However, if sodium citrate is added with caustic as a secondary process aid, the distribution curve shifts significantly to the right to the large size region, especially for the bitumen droplets with sizes greater than 200 μm . This shows that sodium citrate could have

a beneficial effect when synergizing with caustic addition, which leads to a dramatic promotion on bitumen droplet size increase.

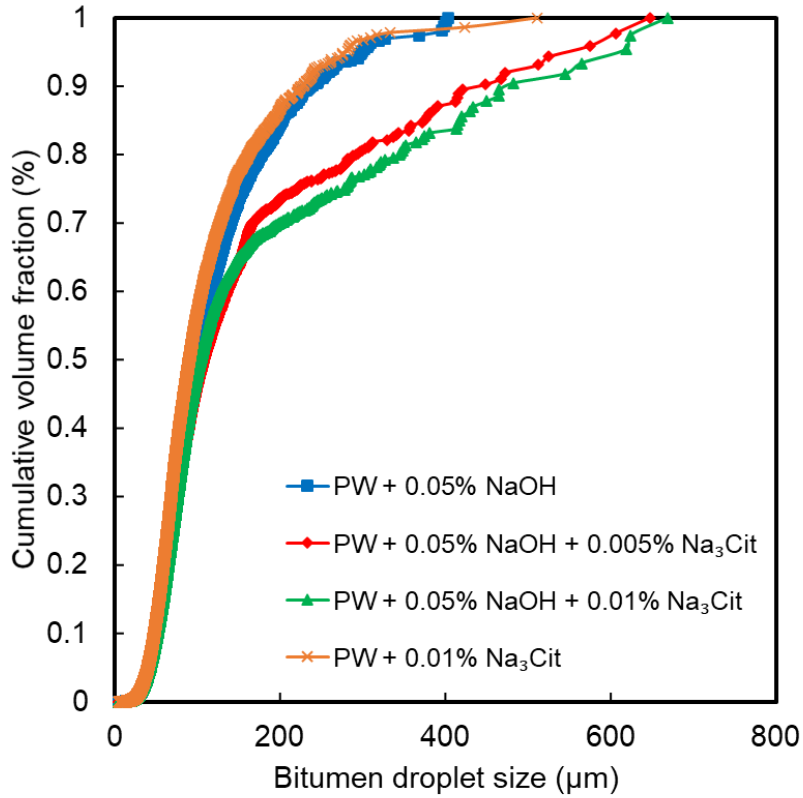


Figure 11. Cumulative bitumen droplet size volume-based fraction in the presence of caustic and sodium citrate.

Figure 12 shows a detailed histogram of the volume fraction of bitumen droplets in different size ranges. From 0 to 100 µm, the percentage of bitumen droplets among all chemical addition in this size range is relatively similar, except for the case of sodium citrate alone. In the case of adding sodium citrate alone in process water, there is a 3% and 6% difference between the sodium citrate alone group and other groups at the 0 - 50 µm and 50 - 100 µm range. This indicates that there are more small droplets in the slurry with the addition of sodium citrate alone. From 100 - 250 µm, the cases with caustic and sodium

citrate alone show a higher percentage of bitumen droplets located in this size range; while from 250 - 300 μm , all four cases have a similar percentage of bitumen droplets. However, at the size range greater than 300 μm , the percentage of bitumen droplets is much higher with the addition of caustic and sodium citrate together ($\sim 18\%$ compared to $\sim 3\%$ with the addition of caustic and sodium citrate alone). This interesting phenomenon shows that neither the caustic nor sodium citrate alone can promote bitumen droplet size growth, but if they are added together, they can synergistically promote bitumen droplet size increase. The synergistic effect works mainly on medium-sized bitumen ranging from 100-250 μm , which help median sized droplets to coalesce into droplets bigger than 300 μm .

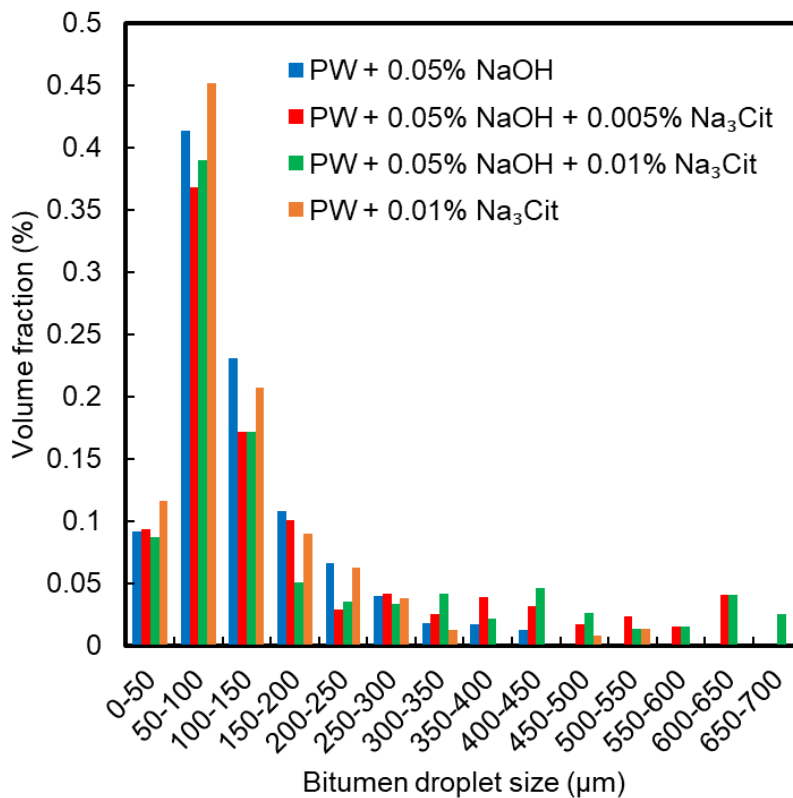


Figure 12. Histogram of bitumen droplet size distribution with caustic and sodium citrate.

3.2.3. Bitumen droplet size as a function of time

This experiment is designed to investigate whether the increase of bitumen droplet size is due to the bitumen coalescence as we proposed, or because the bitumen liberated from sand grains becomes larger with citrate addition.

Liberation usually happens at the initial stage of hydrotransport. From previous research, sodium citrate as a SPA can significantly increase liberation.^{2,5} Therefore, it is possible that the observed large bitumen droplets were liberated from oil sands directly.

As shown in previous research, a higher pH condition is favourable for liberation and detrimental for bitumen droplet coalescence.^{2,10} If bitumen droplets are liberated as small droplets, then at that pH value, the coalescence of droplets is highly unlikely due to the high EDL repulsion between the droplets. However, due to the shear caused by stirring, there is still a chance that mechanical energy could help a small number of bitumen droplets to coalesce, but the bitumen droplet size should be relatively constant.

As shown in Figure 13, with 0.05 wt.% caustic alone (pH ~ 10), bitumen droplet size distribution was relatively stable at all 4 time points. The values of D90 and D50 only exhibited negligible changes from 5 to 30 minutes (Figure 15). D90 has raised from around 200 μm to 220 μm from 5 to 10 minutes, and after that, it increased slowly from around 220 μm to 250 μm at 30 minutes. This slight increase was most likely caused by the shear-induced droplet coalescence.

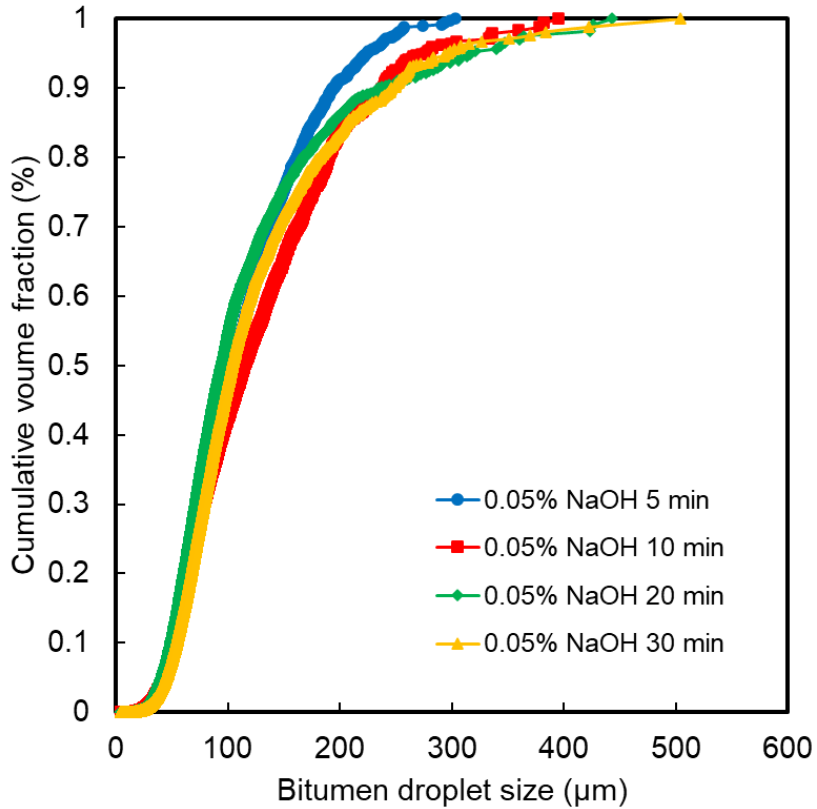


Figure 13. Cumulative volume-based bitumen droplet size distribution with 0.05 wt.% caustic at different mixing times.

However, with 0.05 wt.% caustic and 0.01 wt.% sodium citrate together (pH ~ 9.9), the bitumen droplet size distribution has significantly shifted toward a bigger size zone from 5 to 30 minutes (Figure 14). D50 was relatively stable, but D90 has grown rapidly from ~ 200 µm at 5 minutes to around 480 µm at 30 minutes, which is more than doubled in size (Figure 15). It is known that adding sodium citrate does not change the pH dramatically. Therefore, the previous conditions of better liberation and poorer coalescence are still valid after adding sodium citrate based on high pH. However, bitumen droplet size increased after adding sodium citrate as a SPA with caustic, and the size grew as a function

of time. This phenomenon should thereby be attributed to the synergistic effect between citrate and caustic, which facilitates the bitumen coalescence.

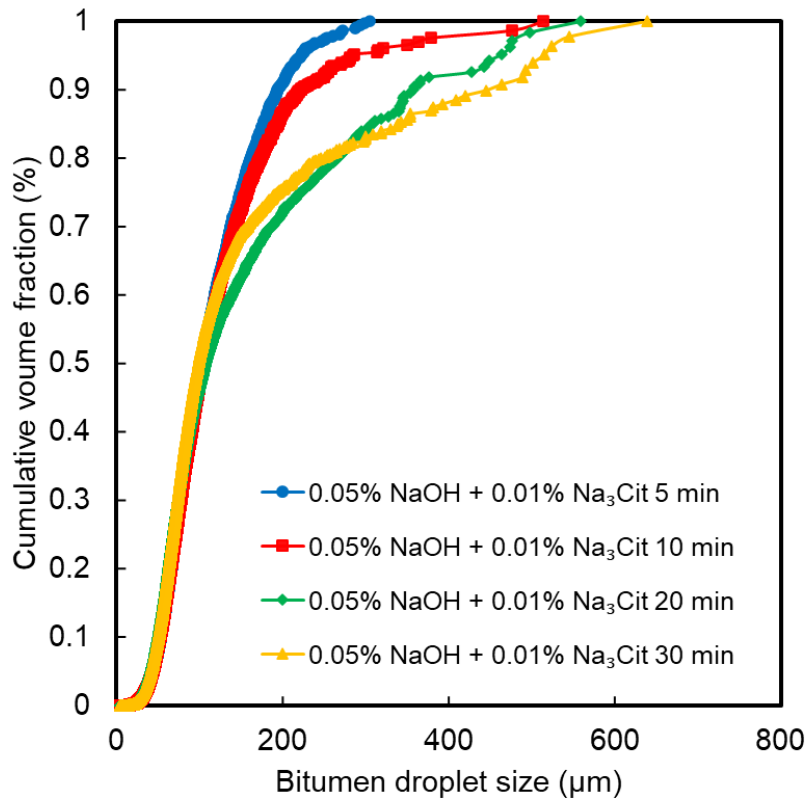


Figure 14. Cumulative volume-based bitumen droplet size distribution with 0.05 wt.% caustic and 0.01 wt.% sodium citrate at different mixing times.

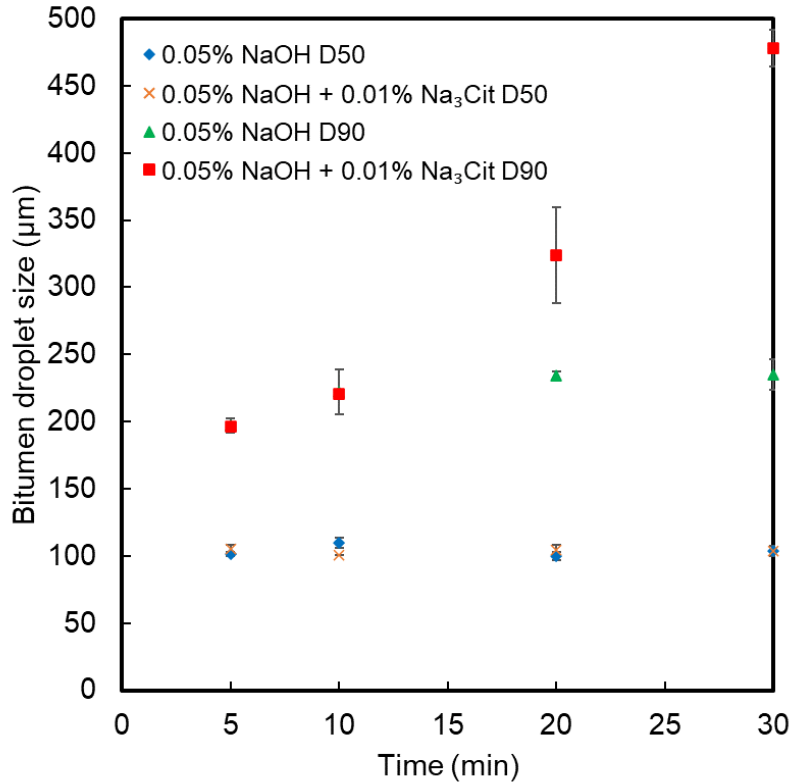


Figure 15. Bitumen droplet size (D90, D50) as a function of time with 0.05 wt.% caustic alone and with 0.01 wt.% sodium citrate as SPA.

It can be concluded that the increase of bitumen droplet size is a result of enhanced bitumen coalescence. If the growth was mainly due to liberation, big droplets should exist from the beginning instead of growing over time. Besides, if growth was mainly due to liberation, a similar but slightly worse pattern should also be observed with caustic alone. Adding caustic alone already increases liberation recovery, while sodium citrate works as a secondary process aid to help the liberation process. Interestingly, the two D90 curves followed a similar growth trend and number from 5 to 10 minutes. Liberation during this time period may help the number of liberated bitumen droplets in the slurry increase, which could result in higher collision efficiency and higher coalescence rate. But after 10 minutes,

bitumen droplet size increased significantly with sodium citrate as a SPA. Based on the previous discussion, the dramatic increase should be mainly due to droplet coalescence, and sodium citrate as SPA could help the droplet coalescence process.

3.2.4. Summary

In the oil sands system, adding caustic alone or sodium citrate alone did not promote bitumen droplet size increase. However, if sodium citrate was added as a secondary process aid together with caustic, it had a synergistic effect on bitumen droplet size growth.

The growth may not be related to better liberation caused by sodium citrate, which could possibly liberate bigger bitumen droplets. The growth is more likely due to bitumen droplet coalescence in the medium-sized zone range of 100 - 250 μm . Therefore, the focus of future research should be on how sodium citrate affects bitumen droplets coalescence.

4. Effect of sodium citrate on bitumen droplet size in model bitumen emulsion system with process water

4.1. Methodology

4.1.1. Materials

Vacuum stillied bitumen from Canada Syncrude Inc. was used to prepare bitumen emulsions in this chapter. Sodium citrate (from Fisher Scientific) at 0.1, 0.5 and 1 mM concentrations were added into process water (pH ~ 8.5) before or after making an emulsion.

4.1.2. Experiment method

SOPAT is a photo-optical and image-based analysis measurement technology. It is used to take photos and analyze particle size distribution and characteristics in multi-phase systems. As shown in Figure 16, SOPAT takes photos and detects droplets in the photos. The shape and characteristics of bitumen droplets can be then analyzed by the accompanied software.

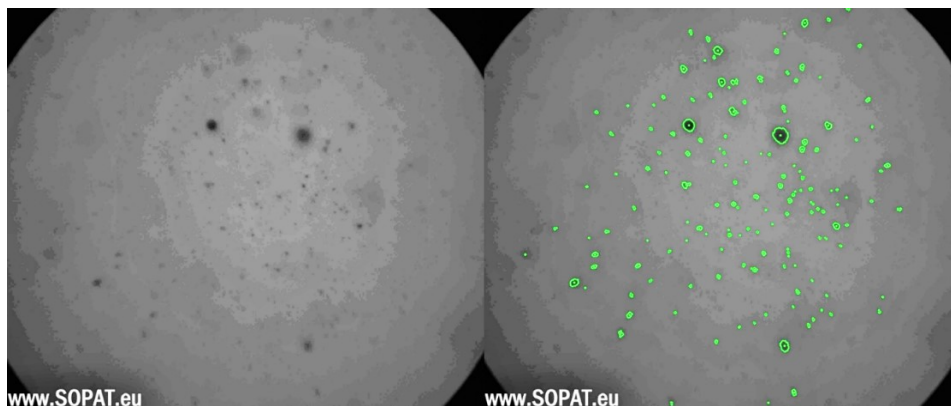


Figure 16. Use of SOPAT to detect bitumen droplets. Left: Original image. Right: Analyzed image.

The procedure for preparing bitumen-in-water emulsions is schematically shown in Figure 17. Bitumen samples of 1 wt.% were emulsified in 40 mL of the aqueous solution of desired water chemistry using an ultrasonic dismembrator. The resultant bitumen emulsion was then transferred into a beaker with the SOPAT probe. To reduce the chance of bitumen droplet sticking on the stir bar, a glass stir bar was soaked in pH 12 NaOH solution for 10 minutes to hydrophilize its surface. Then, the pre-treated glass stir bar was put inside the beaker with a stirring speed of 100 rpm. Then, the particle size in the emulsion was measured by 50 frames per second (FPS) in 1-minute increments for 30 min to monitor the coalescence behaviour of the bitumen emulsion.

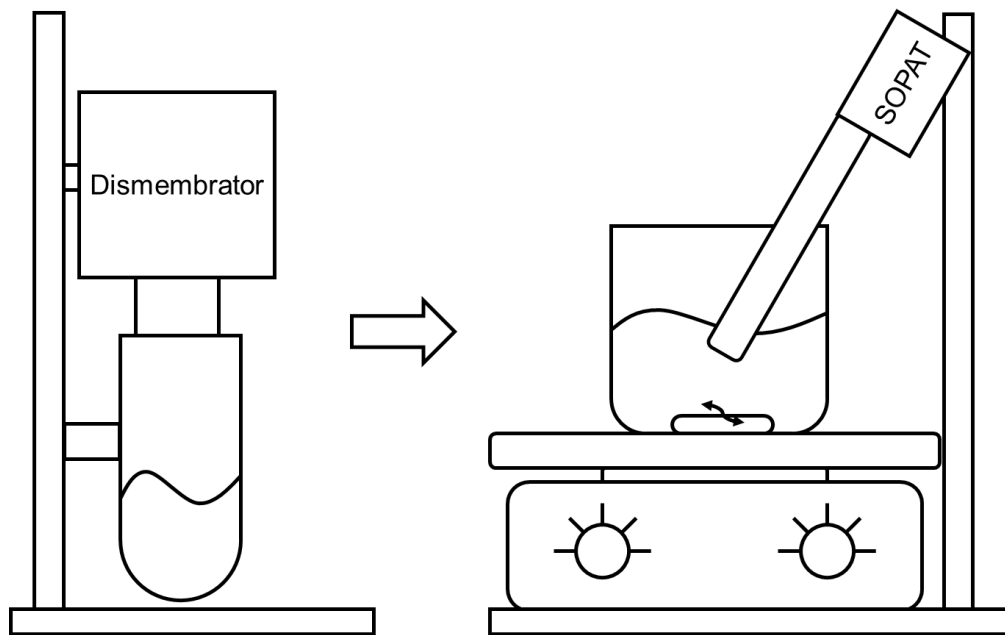


Figure 17. Experiment set up for bitumen droplet size measurement with SOPAT.

This bitumen droplet size measurement experiment was done in 3 sets:

(1) 40 mL of process water was added into a cell together with 0.4 g bitumen and 0.1, 0.5 or 1 mM sodium citrate. The cell was transferred and installed on the dismembrator.

Dismembrator was operated with a 70% amplitude for 30 minutes. After that, the bitumen emulsion inside the cell was transferred to a 100 mL beaker. Then, the stir bar started to stir at 100 rpm. The SOPAT test was then conducted for a duration of 30 minutes.

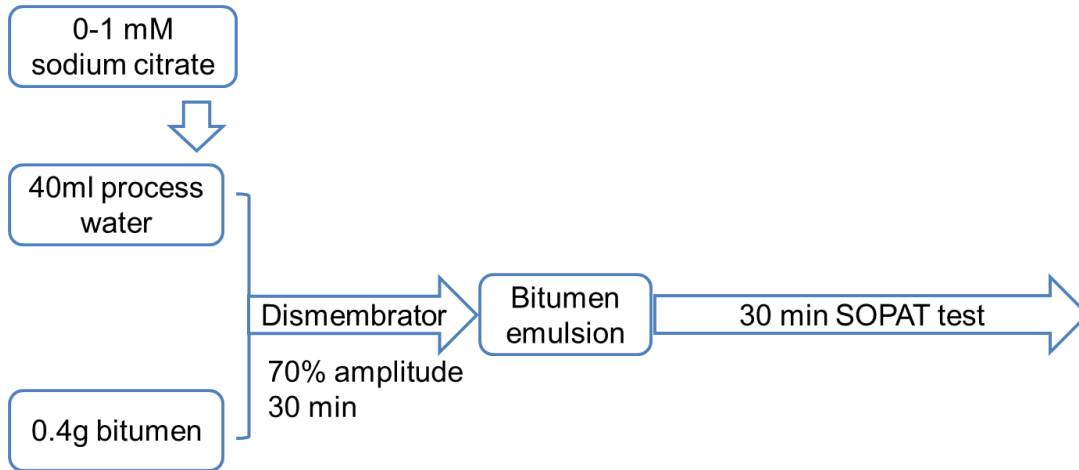


Figure 18. Procedure of the set 1 experiment with process water.

(2) 40 ml process water was added into a cell together with 0.4 g bitumen. After the bitumen was made and transferred to the beaker, 0.1, 0.5, or 1 mM sodium citrate was added inside the emulsion. The remaining procedure was the same as in 4.1.2 (1).

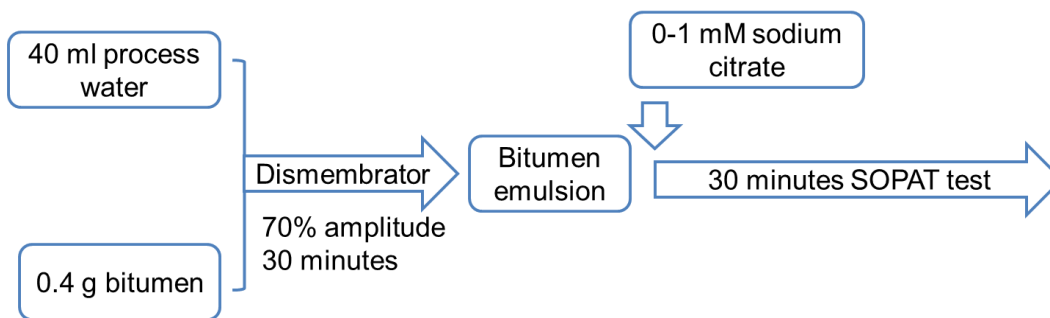


Figure 19. Procedure of the set 2 experiment with process water.

(3) 40 ml process water was filtered by a 0.22 μm syringe filter first, in order to remove fines contents in the process water. Then, the filtered process water was mixed with 0.4 g bitumen into a cell. The remaining procedure was the same as in 4.1.2 (2).

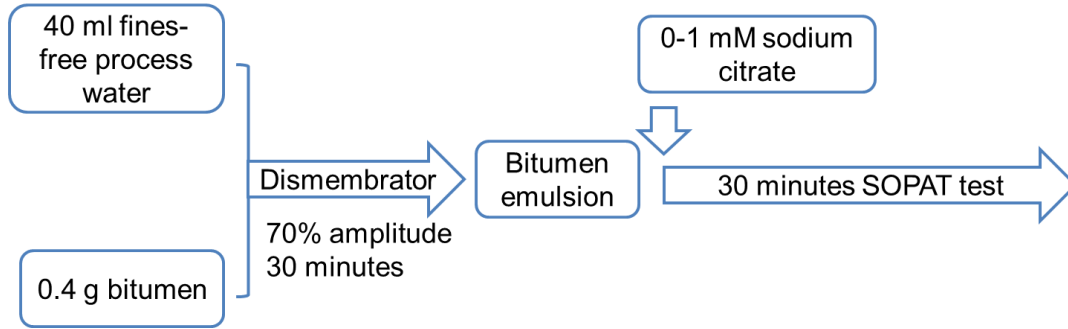


Figure 20. Procedure of the set 3 experiment with process water.

4.2. Results and discussion

4.2.1. Effect of sodium citrate in process water (citrate pre-added)

In experiment set 1, sodium citrate was pre-added into process water, which is similar to the procedure in Chapter 3. The results are shown in Figure 21 and there exist both similarities with and differences from the results in Chapter 3.

In all four cases, the bitumen droplet size increased with time, but at different magnitudes (Figure 22). Bitumen droplet size increased the most with 0.1 mM sodium citrate addition in process water, growing from around 45 μm to 100 μm . For the process water scenario, bitumen droplet size grew from around 50 μm to 80 μm . The result showed that adding 0.1 mM sodium citrate helped bitumen droplet size increasing more significantly. The beneficial effect of sodium citrate shown above is consistent with the results from Chapter 3.

However, when sodium citrate was added with concentrations of 0.5 mM and 1 mM, the growth ($\sim 40 \mu\text{m}$ to 60 μm and ~ 40 to 55 μm , respectively) was not as pronounced

as in process water. This phenomenon is opposite to the result in Chapter 3. It shows that adding a relatively high dosage of sodium citrate could hinder the increase of bitumen droplet size. Previous research has shown sodium citrate can increase the absolute value of zeta potential of bitumen droplets, and the resulting higher EDL repulsion can prevent attachment between bitumen and sand.^{5,49,77} For two negatively charged bitumen surfaces, the EDL repulsion increases when adding more sodium citrate. At a certain dosage, the EDL repulsion might be able to prevent bitumen droplets coalescence, resulting in a smaller bitumen droplet size. The result showed that sodium citrate has a beneficial effect on bitumen droplet size growth but at a relatively low concentration. When the concentration was high, sodium citrate had a negative effect on the size growth, which may be due to high EDL repulsion. Therefore, there is likely an optimum sodium citrate concentration for the best coalescence performance in process water, which is around 0.1 mM in this experimental condition.

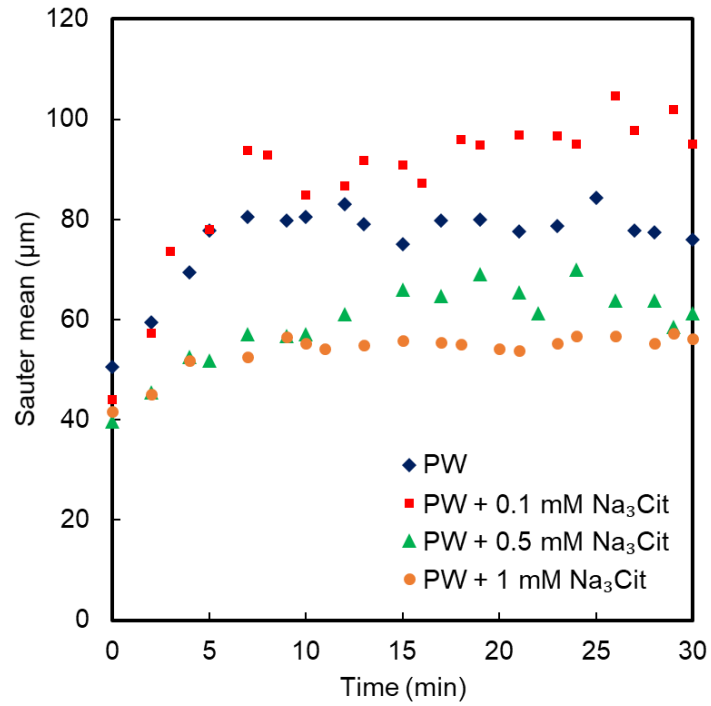


Figure 21. Evolution of the bitumen droplet Sauter mean size in Na₃Cit pre-added process water.

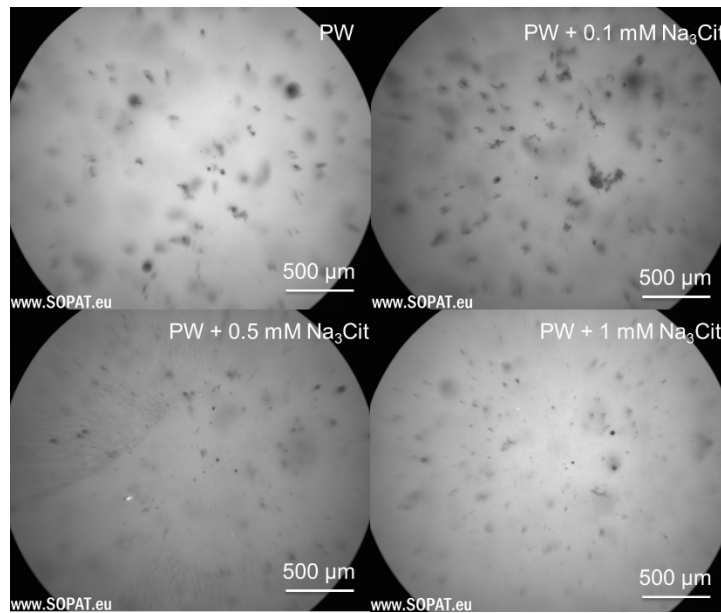


Figure 22. Bitumen emulsion images taken by SOPAT in Na₃Cit pre-added PW with 0-1 mM sodium citrate.

4.2.2. Effect of sodium citrate in process water (sodium citrate post-added)

In experiment set 2, the bitumen emulsion was made without pre-added sodium citrate. 0 - 1 mM sodium citrate was added before stirring. As shown in Figures 23 and 24, in process water, the bitumen droplet size decreased with increasing sodium citrate concentration. Without sodium citrate, the bitumen droplet size grew from around 50 μm to 80 μm . However, the bitumen droplet size only grew from 50 μm to slightly below 60 μm with the presence of sodium citrate. Regardless of the dosage of sodium citrate, all cases had negative effects on bitumen droplet size growth. This different phenomenon compared to set 1 should be a consequence of adding sodium citrate.

One of the major concerns when using industrial process water is the presence of fine clay particles, which might change the colloidal interactions. During emulsification, clay particles might attach to the bitumen droplet surface and cause slime coating. Previous research has shown that the addition of sodium citrate can prevent slime coating.⁷⁷ However, it has to be mentioned that the same study also demonstrated that sodium citrate could not remove the slime coating that had already happened.⁷⁷ In the current experimental setup (as shown in Figure 19), it is possible that slime coating may have already happened during emulsification if there were fine particles existing in the process water, and the clay layer on the bitumen surface could prevent the coalescence process. With the synergetic effect of a more negatively charged surface caused by sodium citrate, the strong repulsion also prevents bitumen droplets from coalescing.

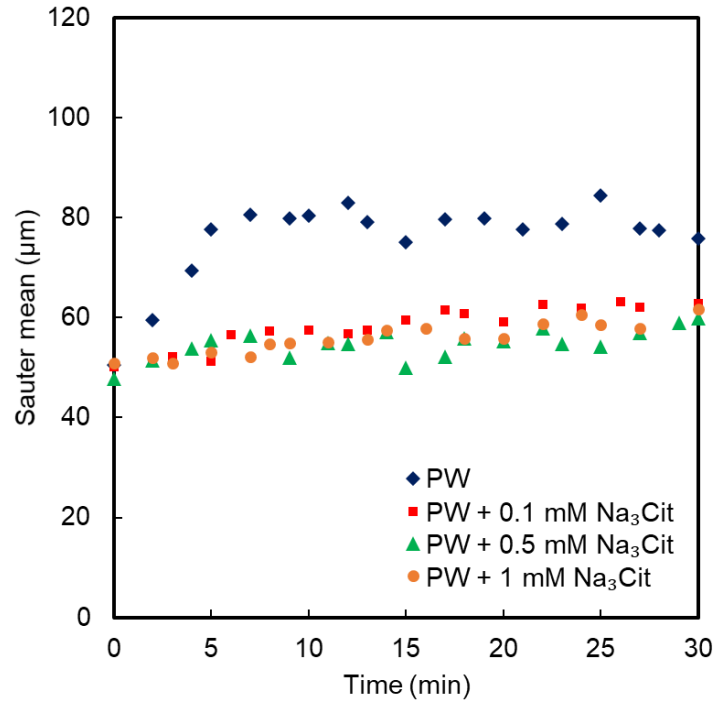


Figure 23. Evolution of the bitumen droplet Sauter mean size in Na₃Cit post-added process water.

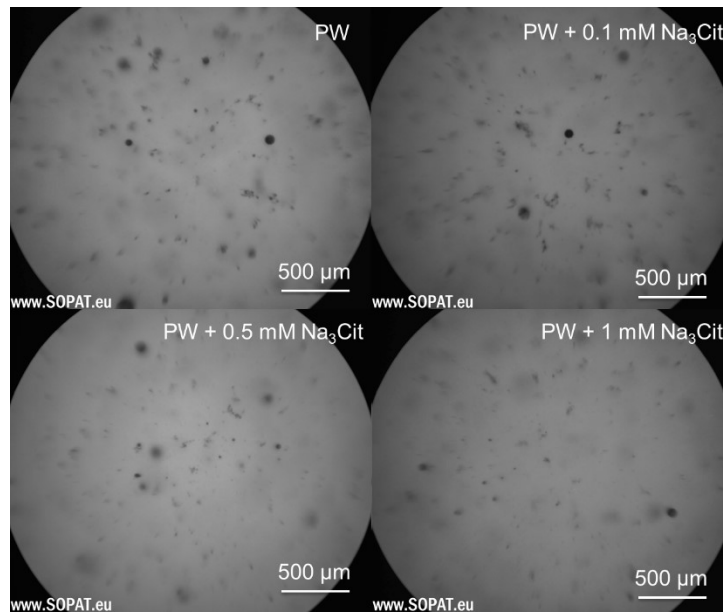


Figure 24. Bitumen emulsion images taken by SOPAT in Na₃Cit post-added PW with 0-1 mM sodium citrate.

4.2.3. Effect of sodium citrate in fines-filtered process water

From the previous sections, it can be seen that fines may play a detrimental role in bitumen droplet size growth. As a result, the slime coating phenomenon might prevent sodium citrate from achieving its beneficial effect on bitumen droplet size growth. Therefore, experiment set 3 was designed to prepare bitumen emulsions under a fines-filtered process water environment, such that little slime coating effect would be considered. In this manner, the effects of sodium citrate on bitumen coalescence can be studied explicitly.

As shown in Figures 25 and 26, the overall trend of sodium citrate on bitumen droplet size evolution in fines-filtered process water is similar to that in experiment set 1 (Figure 21). There exists an optimum dosage of sodium citrate to achieve the biggest droplet size growth, which is 0.1 mM. With 0.1 mM sodium citrate added, bitumen droplet size grew from around 40 μm to 100 μm . For the cases with only process water, 0.5 mM and 1 mM sodium citrate addition, bitumen droplet size growth trends were similar, from around 40 μm to 60 μm .

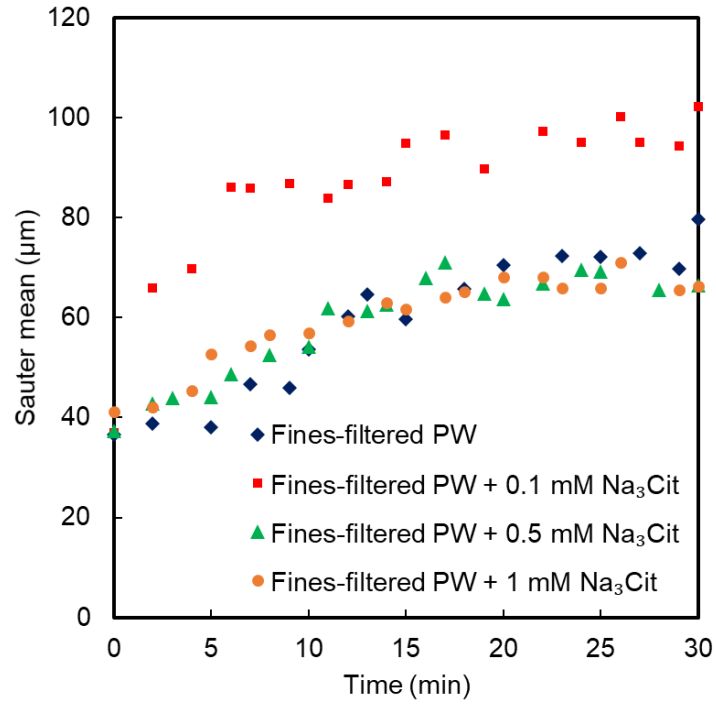


Figure 25. Evolution of the bitumen droplet Sauter mean size in fines-filtered process water.

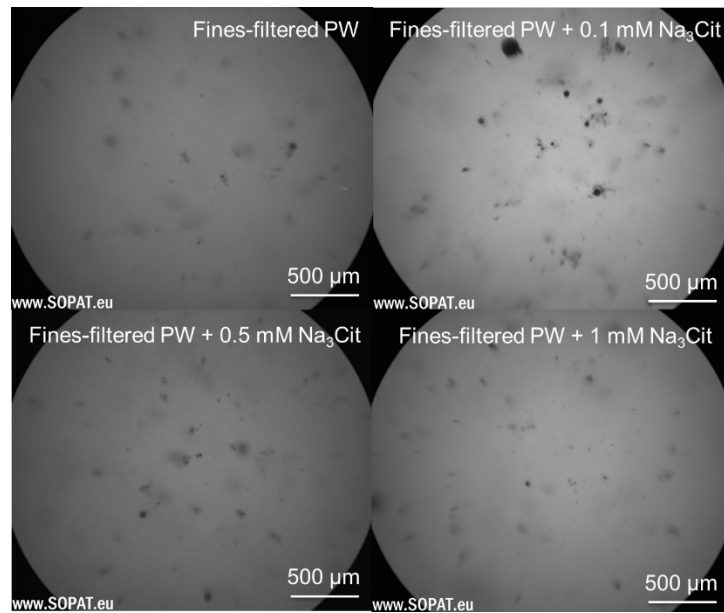


Figure 26. Bitumen emulsion images taken by SOPAT in fines-filtered PW with 0-1 mM sodium citrate.

4.2.4. Comparison between the cases with process water and discussion

From the previous sections, sodium citrate showed different effects based on the fines content in process water and the sequence of adding sodium citrate. As shown in Figure 27, if sodium citrate was added after the emulsion was made in process water, it had a completely different effect compared to fines-filtered process water and citrate pre-added process water. Without sodium citrate, bitumen droplet size grew by around 30 μm , but the growth shrank to only around 10 μm with any dosage of sodium citrate.

If fines were removed from process water, the bitumen droplet size increased by around 38 μm without sodium citrate. The size growth increased by 60 μm with 0.1 mM sodium citrate, which almost doubled the original growth. However, the growth dropped to around 35 μm with 0.5 mM or 1 mM sodium citrate addition, which is almost negligible to the cases without addition.

If sodium citrate was pre-added into process water before emulsification, it promoted droplet size increase, but at a smaller magnitude. For example, the growth was around 55 μm with 0.1 mM sodium citrate addition, which is higher than in sodium citrate post-added process water, but lower than in fines-filtered process water.

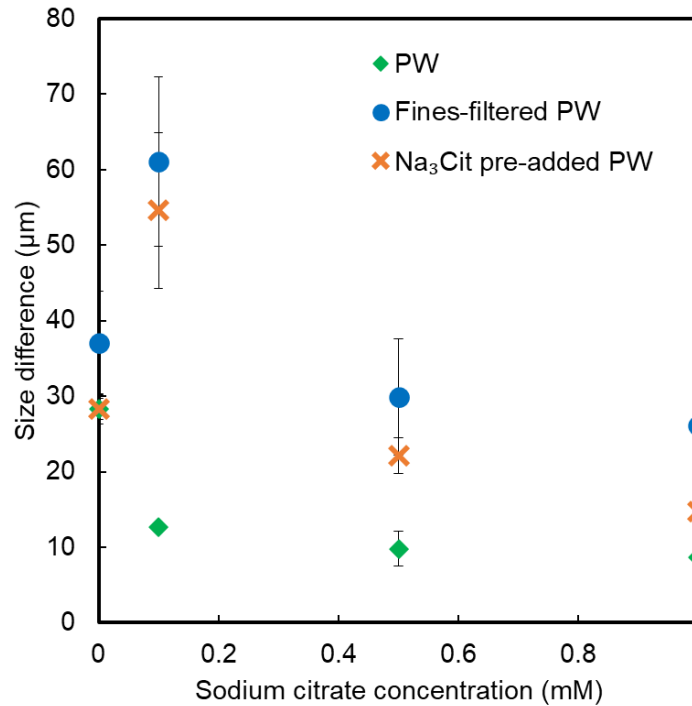


Figure 27. Bitumen droplet size difference between 0 minutes and the average of the last 5 minutes in PW, fines-filtered PW, and sodium citrate pre-added PW.

From the above comparison, it can be confirmed that the effectiveness of sodium citrate on promoting bitumen droplet size growth depends on at least 3 factors: sodium citrate concentration, sodium citrate adding sequence, and fines concentration.

For sodium citrate concentration, there seems to exist an optimum dosage for bitumen droplet size growth. It is obvious that if EDL repulsion increases with increasing sodium citrate concentration, the chance for bitumen droplet coalescence decreases as a consequence. As a result, the bitumen droplet size should always decrease with increasing sodium citrate concentration by only considering the surface forces. However, the results show bitumen droplet size difference first increases at low sodium citrate concentration

and then decreases at relatively higher sodium citrate concentration. Therefore, there must be some other factors contributing to the beneficial effect of sodium citrate.

Although the current evidence supports that sodium citrate has a beneficial effect at the optimum dosage, such a favourable phenomenon has one prerequisite condition, which is the elimination of slime coating. Adding sodium citrate before emulsification can prevent slime coating from happening, but not completely. Therefore, the overall slime coating degree is significantly reduced compared to adding sodium citrate after emulsification. Since there are still fines attaching to bitumen, the overall slime coating degree when pre-adding sodium citrate is slightly higher than in fines-filtered process water. The size increase is the biggest in fines-filtered process water. While in sodium citrate pre-added process water, the size increase is slightly lower. In sodium citrate post-added process water, the size increase is the least among all three conditions.

Therefore, it is obvious that bitumen droplet size is negatively affected by the degree of slime coating. Sodium citrate could have a beneficial effect on bitumen droplet size by controlling the slime coating degree.

4.3. Effect of sodium citrate on clay on the bitumen droplet surface

From the results in Chapter 3 and the discussion in Chapter 4.2, it is demonstrated that one of the mechanisms of sodium citrate affecting bitumen droplet coalescence has to be related to the clay. If sodium citrate was added before the slime coating happens, sodium citrate can effectively prevent slime coating from happening. Otherwise, slime coating could not be removed if sodium citrate was added after slime coating already happened.⁷⁷

Therefore, it is essential to prevent slime coating first, a step that is key to obtaining the positive effect of sodium citrate on enhancing bitumen droplets coalescence. If slime coating happens first, the beneficial effect of sodium citrate would not become evident and the impact can even be negative. In the oil sands system, this prevention step is also of extreme importance due to the presence of much higher fines concentration. As shown in Figure 28, the bitumen surface may be partially covered by clay before liberation happens. With the synergistic effect of caustic and sodium citrate, a better liberation can be achieved. Meanwhile, sodium citrate can prevent further slime coating from happening on the clean bitumen surface just liberated from the sand surface. Those clean surfaces can interact with other clean surfaces and eventually form aggregate and bigger droplets.

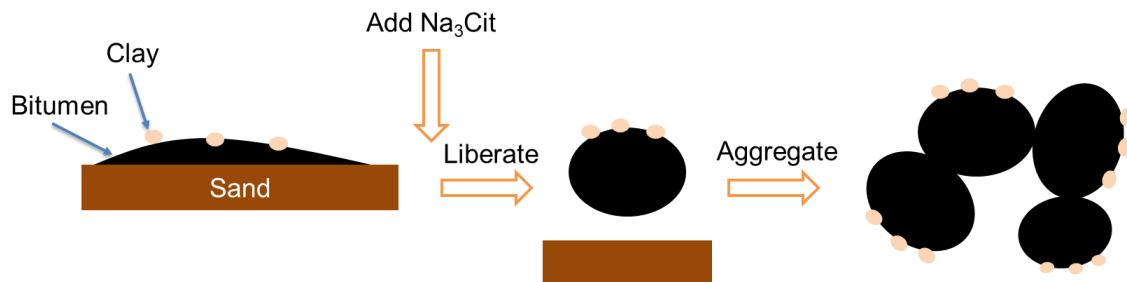


Figure 28. Possible mechanism of sodium citrate helping to prevent slime coating and promoting bitumen droplet coalescence.

4.4. Summary

Sodium citrate has shown a beneficial effect at an optimum dosage (0.1 mM in this study) on droplet size growth when it was pre-added into process water or added into fines-filtered process water. If sodium citrate concentration was higher than the optimum dosage (> 0.5 mM), it did not exhibit a beneficial effect on droplet size increase. When sodium

citrate was post-added into process water, it had a significant negative effect on droplet size at all concentrations.

This phenomenon is most likely related to the manipulation of slime coating. In fines-filtered process water, where little slime coating could happen, sodium citrate has a beneficial effect at 0.1 mM. However, it does not have any beneficial effect when post-added into process water, where slime coating has already occurred. Once sodium citrate prevented slime coating when pre-added, it showed the beneficial effect again. Therefore, the prevention of slime coating is a prerequisite condition to enable the beneficial effect of sodium citrate on bitumen droplet coalescence in process water.

5. Effect of sodium citrate on bitumen droplet size in model bitumen emulsion system with synthetic water

5.1. Methodology

5.1.1. Materials

Vacuum distilled bitumen was provided by Canada Syncrude Inc. Synthetic process water was made with DI water, and it contained the salts in Table 4.⁷⁸ The pH of synthetic process water was controlled at 8.5 by titrating NaOH/HCl.

Table 4. Synthetic process water recipe.

| Salt | Concentration (mM) |
|---------------------------------|--------------------|
| Na ₂ SO ₄ | 2.10 |
| NaHCO ₃ | 12.49 |
| NaCl | 9.05 |
| CaCl ₂ | 1.10 |
| MgCl ₂ | 0.78 |

Calcium chloride, sodium citrate and sodium hydroxide were analytical degrees and were purchased from Fisher Scientific.

5.1.2. Experiment set up

5.1.2.1. Bitumen droplet size measurement

SOPAT and FBRM were used to measure bitumen droplet size in this chapter. Focused beam reflectance measurement (FBRM) and Smart online particle analysis technology (SOPAT) were used to measure the size distribution of bitumen droplets in various aqueous solutions. FBRM is one of the most flexible equipment to measure

particles with a measurement range of 0.5 - 2000 μm . FBRM uses a rotating laser to measure the chord length distribution (CLD) of the particles. Schümann⁷⁹ compared particle video microscopy (PVM) with FBRM and presented a method to convert obtained CLDs to particle size distributions (PSD). Boxall measured oil, crude oil, and mineral oil with FBRM, which means FBRM is able to measure bitumen droplet emulsions.²¹

The current experiments to measure the bitumen droplet size were done in 3 steps. In the first step, the bitumen droplet size was measured in DI water and single ions with FBRM. In the second step, bitumen droplet size was measured in DI water and multiple ions with FBRM. In the third step, bitumen droplet size was measured in synthetic process water with SOPAT.

When using the FBRM method (Figure 29), 1 wt.% vacuum distillation bitumen was emulsified in 30 mL of the aqueous solution of desired water chemistry with an ultrasonic dismembrator. Then, the emulsion was diluted with the same amount of the aqueous solution to satisfy the volume requirements of the FBRM measurement. The resultant bitumen emulsion was added to a beaker with the FBRM probe inserted at 45 degrees from the vertical line. A stirrer motor was installed on the top of the beaker and an impeller was attached and inserted into the emulsion with a stirring speed of 100 rpm. Then, the particle size in the emulsion was measured in 10 s increments for 30 min to monitor the coalescence behaviour of the bitumen emulsion.

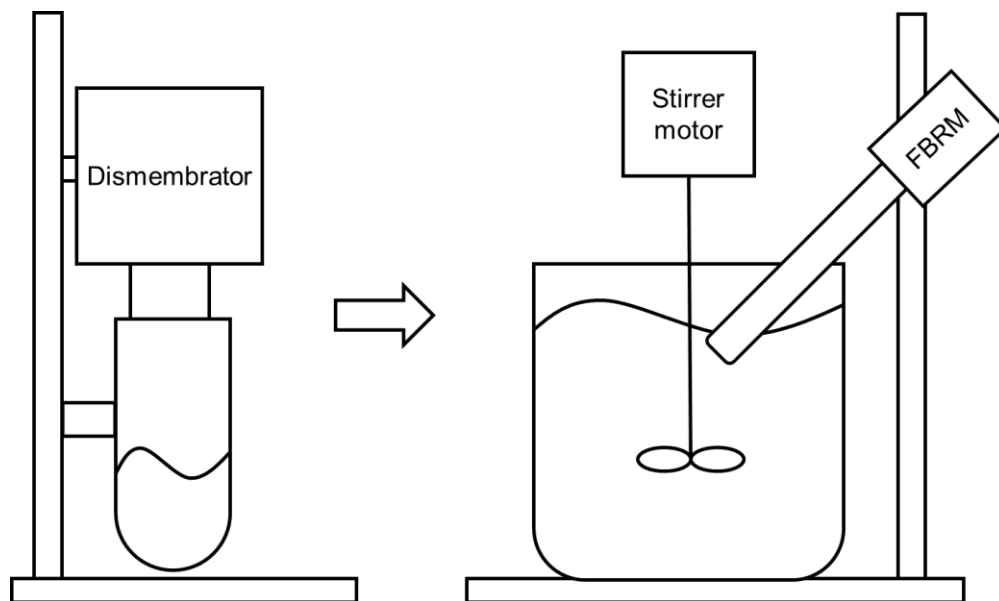


Figure 29. Experimental set up for bitumen droplet size measurement with FBRM.

The experiments using SOPAT followed similar methods as in Chapter 4. The experiments were conducted with the sets below:

1) Set 1: As shown in Figure 30, the bitumen emulsion was prepared with 1 wt.% bitumen and pH 8.5 sodium hydroxide solution. 0.1 mM, 0.5 mM, or 1 mM calcium chloride, or sodium citrate were added separately to investigate the effect of different chemicals individually. The maximum concentration for divalent ions in the industry is around 1 mM. Therefore, the concentration for this experiment was chosen to be in the industrially relevant range.

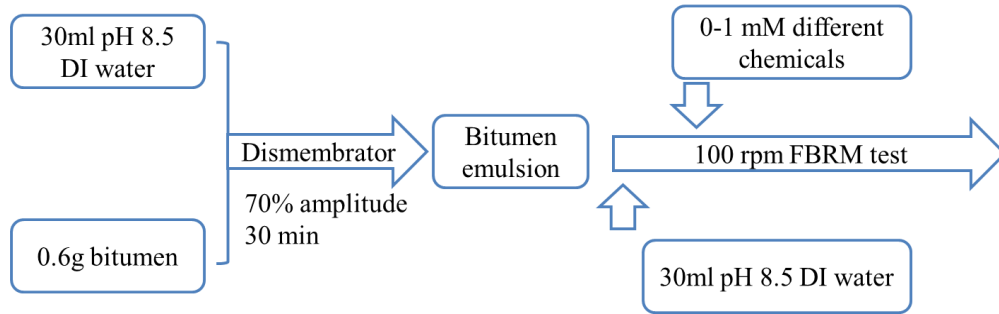


Figure 30. Procedure of the set 1 experiment with synthetic water.

2) Set 2: As shown in Figure 31, the bitumen emulsion was made by mixing 1 wt.% bitumen and pH 8.5 sodium hydroxide solution with 0.1 mM to 1 mM calcium chloride. 0.1 mM, 0.5 mM, or 1 mM sodium citrate was added to investigate the effect of sodium citrate with the presence of divalent cations, respectively. The chemical concentration for each experiment is listed in Table 5.

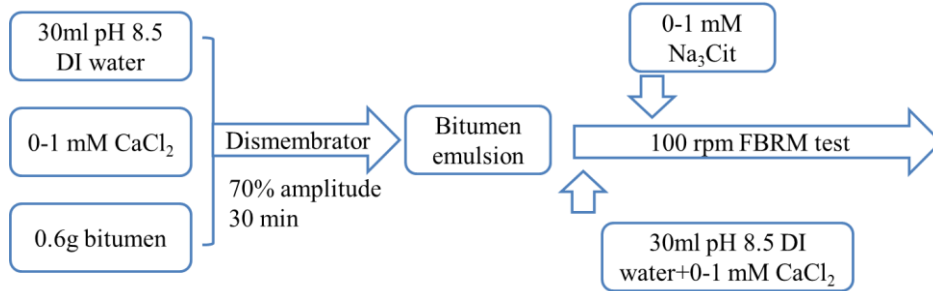


Figure 31. Procedure of the set 2 experiment with synthetic water (adding calcium ions before emulsification).

Table 5. Salt concentration for FBRM experiment with multi-ions.

| Experiment set number | Calcium chloride concentration (mM) | Sodium citrate concentration (mM) |
|-----------------------|-------------------------------------|-----------------------------------|
| 1 | 0.1 | 0.1 |
| 2 | 0.1 | 0.5 |
| 3 | 0.1 | 1 |
| 4 | 0.5 | 0.1 |
| 5 | 0.5 | 0.5 |
| 6 | 0.5 | 1 |
| 7 | 1 | 0.1 |
| 8 | 1 | 0.5 |
| 9 | 1 | 1 |

3) Set 3: As shown in Figure 32, bitumen emulsion was made with 1 wt.% bitumen and synthetic process water. 0.1 mM, 0.5 mM, or 1 mM sodium citrate was added after emulsification to investigate the effect of sodium citrate in bitumen emulsions with synthetic process water to mimic real processing conditions. The same experimental procedure was performed again but keeping the bitumen emulsion at 40 °C.

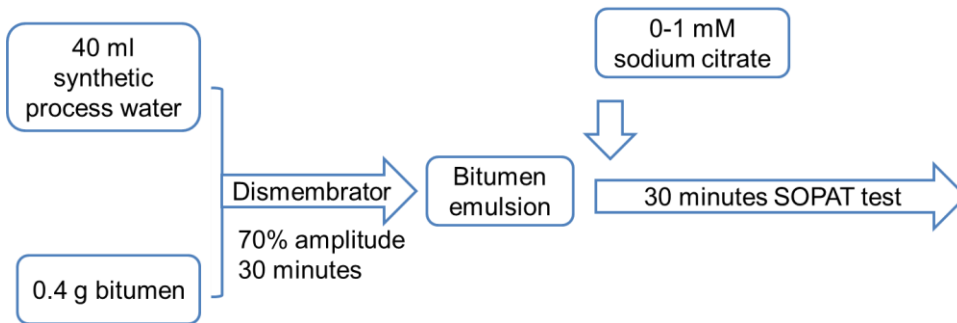


Figure 32. Procedure of the set 3 experiment with synthetic water.

5.1.2.2. Zeta potential measurement

Zeta PALS (Brookhaven) was used to measure the zeta potential of bitumen droplets at room temperature. Bitumen emulsion was made by dismembrator with 1 wt.% bitumen and 30 mL solution with various water chemistry as described previously. Each sample was diluted 10 times with the same solution before it was put into Zeta PALS. Each sample was measured with 5 cycles for a run, and the measurement was repeated for 10 runs.

5.2. Results

5.2.1. Effect of single ions

From Chapters 3 and 4, it was shown that sodium citrate had a beneficial effect on bitumen droplet size growth at a certain optimum dosage. However, those experiments were done with complicated water chemistry. They did not reveal the mechanisms involved with sodium citrate ions alone.

The FBRM result showed that the size of the bitumen droplets was relatively stable during the 30 minutes measurement in a citrate solution, as shown in Figure 33. The size distribution at the beginning and the end of the measurement (Figure 34) show that the droplet size distribution did not have a big difference. This interesting result shows that sodium citrate alone actually prevents bitumen droplet size from increasing.

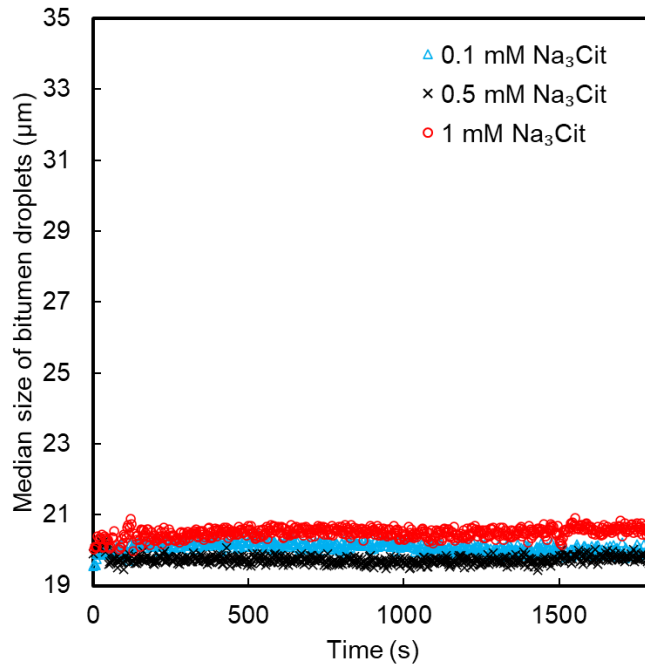


Figure 33. Evolution of median bitumen droplet size in sodium citrate solution.

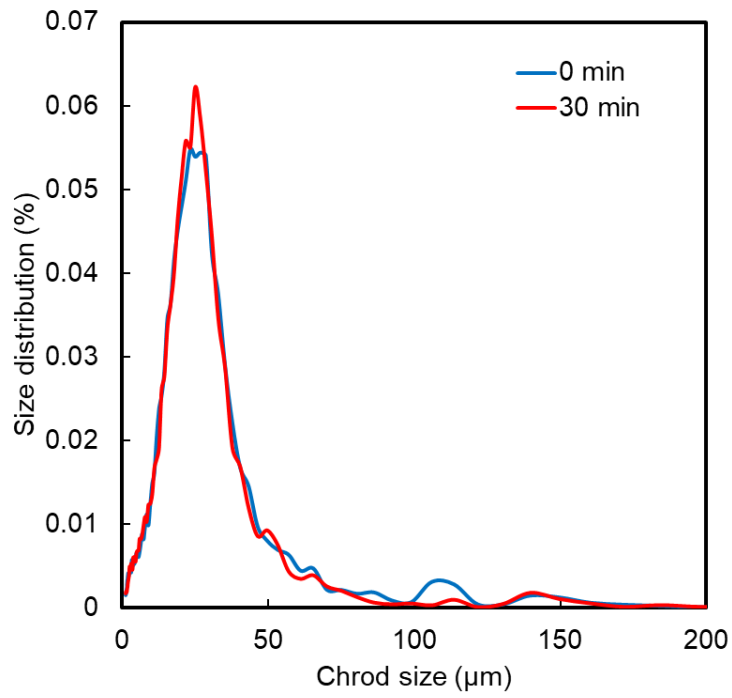


Figure 34. Size distribution chart with the addition of 1 mM sodium citrate.

Divalent ions are known to be troublemakers in the oil sands extraction process. It is hypothesized that sodium citrate could chelate divalent ions to decrease the concentration of “active” divalent ions, thereby improving the liberation process.^{5,77} For bitumen-bitumen interaction, divalent ions have been shown to decrease the repulsion and make attachment easier.¹⁰ FBRM results showed that with the addition of calcium ions, bitumen droplet size increased with increasing calcium ion concentration (Figure 35). From the distribution chart (Figure 36), it can be seen that the distribution significantly shifted to larger sizes with time.

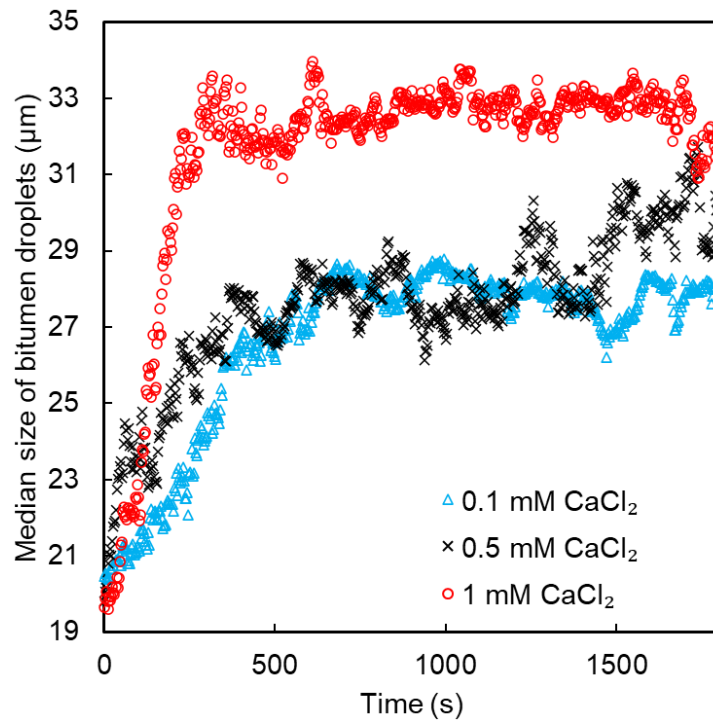


Figure 35. Evolution of median bitumen droplets in calcium chloride solution.

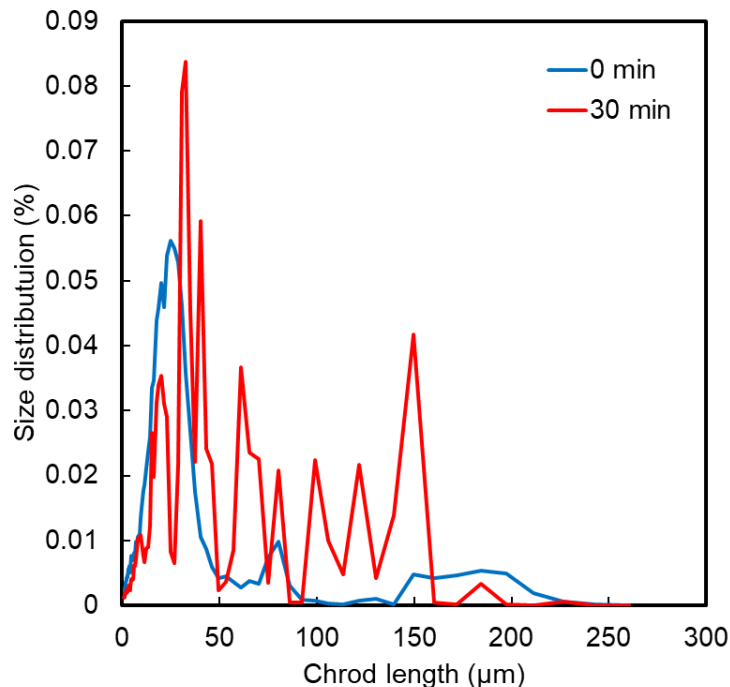


Figure 36. Size distribution chart with the addition of 1 mM calcium chloride.

Consequently, one could conclude that adding calcium ions promotes bitumen droplet size growth, while sodium citrate can prevent bitumen droplet size from growing. Ions in the water can change the bitumen surface zeta potential, which influences the repulsive EDL force. Therefore, the coalescence kinetics of bitumen droplets is significantly affected by water chemistry. Previous research^{5,49} found that the absolute value of the zeta potential of bitumen increased with sodium citrate concentration but decreased with divalent ions. Therefore, the EDL forces should be more repulsive with citrate and less repulsive with divalent ions. This is consistent with the fact that bitumen droplet size increase with calcium ions but not with sodium citrate.

5.2.2. Effect of sodium citrate with divalent ions

In Chapter 4, we demonstrated that sodium citrate had a completely different effect on bitumen coalescence based on the adding sequence. The beneficial effect was only anticipated when sodium citrate was added before emulsification, which may be due to the prevention of slime coating. Calcium chloride played an important role to cause slime coating, and thereby, it links the negatively charged clay particles to the negatively charged bitumen surface. Research has shown that in the presence of calcium ions, slime coating prevention depends on the sequence of adding sodium citrate too.⁷⁷ In this section, fines were not present in the synthetic water, so slime coating would not happen, and the effect of sodium citrate in calcium ions pre-added synthetic water was investigated.

As shown in Figure 37, when calcium ions were added during emulsification, after 30 minutes, bitumen droplet size increases in all sets, and it increases the most with 0.1 mM sodium citrate and 1 mM calcium chloride. With more sodium citrate added, the increased margin was lower.

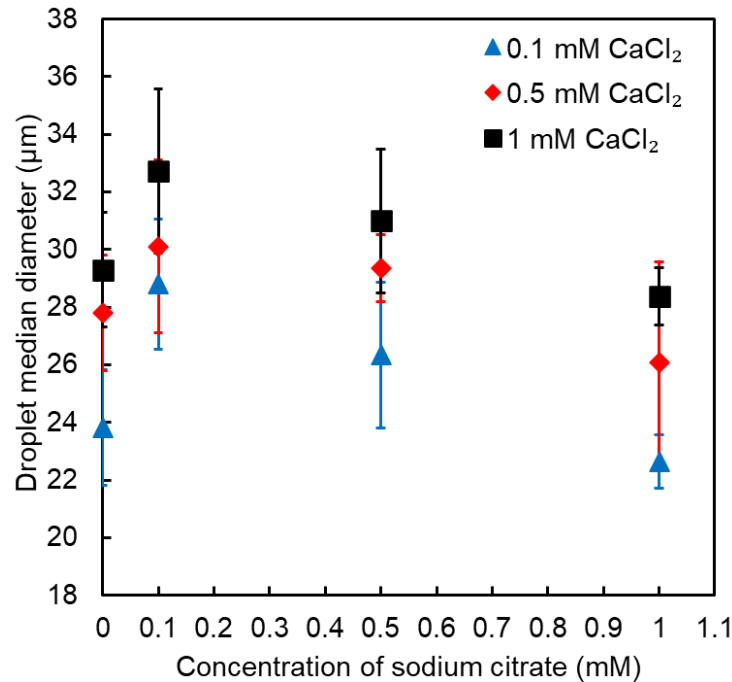


Figure 37. Median bitumen droplet size at 30 minutes as a function of sodium citrate concentration in the presence of calcium ions (adding calcium before making the emulsion, the droplet size among all cases is around $19 \pm 1 \mu\text{m}$ at 0 minute).

Citrate ions can chelate divalent cations, lowering the effective concentration of calcium ions. When sodium citrate was added after the emulsion preparation, some calcium ions had already been adsorbed on the negatively charged bitumen surface. Therefore, the calcium ions effective concentration was readily high at the bitumen surface, because not all sodium citrate had the opportunity to chelate calcium ions. As a result, after chelation, more calcium ions kept adsorbed on the bitumen surface, which kept the surface charge less negative. As a result, sodium citrate can also show its positive effect without significantly lowering surface charge.

At higher concentrations of citrate added to an emulsion containing calcium, it was observed that the bitumen droplet median size dropped with increasing citrate

concentration (Figure 37). However, at 0.1 mM citrate concentration, the bitumen droplet median size was larger than the case where no citrate was added to the Ca^{2+} -containing emulsion. This small amount of citrate may soften the bitumen droplet film. Since the small amount of citrate does not substantially affect the surface charge, the overall surface charge is dominated by calcium ions. Therefore, a combination of less repulsive EDL forces and softer film leads to a higher coalescence probability. Increasing the citrate concentration further has little effect on the film softness but causes an increase in EDL force from the removal of Ca^{2+} from the interface, which results in slower coalescence with an increase of citrate concentration.

5.2.3. Effect of sodium citrate in synthetic process water

Sodium citrate showed similar behaviour in synthetic process water, compared to that in process water, and that in DI water containing divalent ions. The Sauter mean size of bitumen droplet size was the biggest with 0.1 mM sodium citrate. While at higher sodium citrate concentration, the bitumen droplet mean size decreased with increasing sodium citrate concentration (Figure 38). It is obvious that much bigger bitumen droplets can be seen with 0.1 mM sodium citrate in the photo and it forms aggregate (Figure 39).

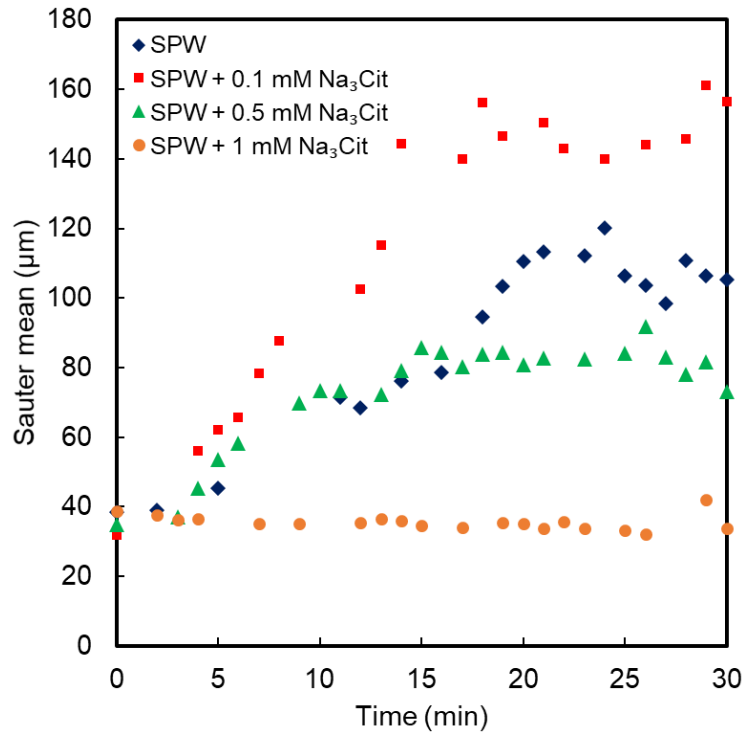


Figure 38. Evolution of Sauter mean bitumen droplet size in synthetic process water.

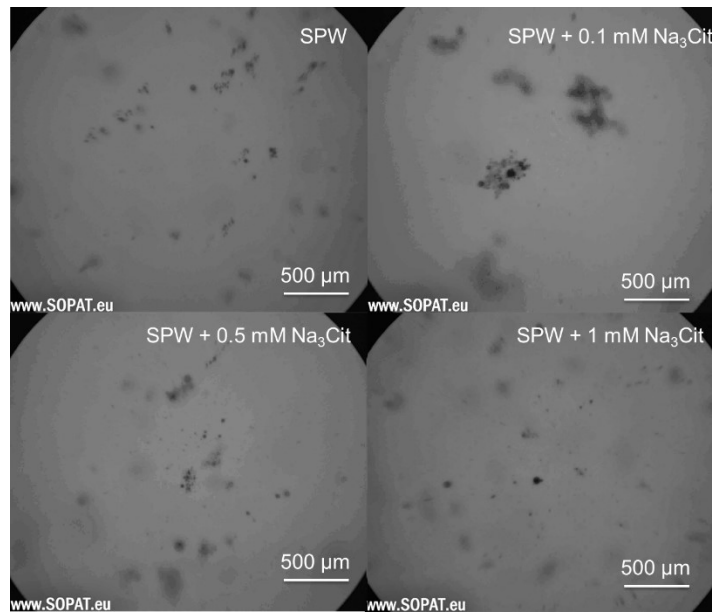


Figure 39. Bitumen emulsion images taken by SOPAT in SPW with 0-1 mM sodium citrate.

Compared with the results from process water, it can be seen that the bitumen droplet size change in SPW followed a similar trend. However, at lower sodium citrate concentration, the margin for size increase was even bigger than in fines-filtered process water and sodium citrate pre-added process water (Figure 40).

Without any sodium citrate, the bitumen droplet size already increased to around 60 μm , which is almost doubled compared to that in fines-filtered process water. This result shows that bitumen droplet size can grow much larger without slime coating. With 0.1 mM and 0.5 mM sodium citrate, the bitumen droplet size growth margin was at least 15 μm more than in any type of process water, which emphasizes again that it is important to prevent slime coating. However, unlike in process water, bitumen droplet did not grow with 1 mM sodium citrate in SPW. Bitumen droplet in SPW has a much cleaner surface without any slime coating, so the effect of sodium citrate may be stronger and more straightforward. Combined with the high EDL repulsion caused by sodium citrate, bitumen droplet size did not increase at this condition.

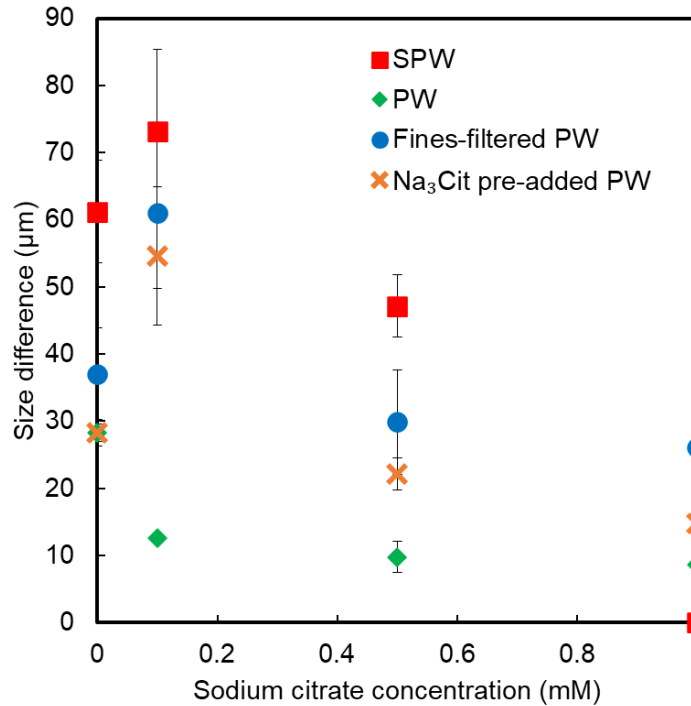


Figure 40. Bitumen droplet size difference between 0 minutes and the average of the last 5 minutes in SPW, PW, fines-filtered PW and sodium citrate pre-added PW.

Previous experiments performed in process water were conducted at 45 °C to mimic the industrial condition. At 45 °C, the viscosity of bitumen drops, and better overall recovery can be achieved. Experiments with synthetic process water were also done at 45 °C to see if sodium citrate performs differently at different temperatures. As shown in Figure 41, the coalescence rate increased at 45 °C. It only took 10 minutes to reach a relatively stable condition of bitumen droplet sizes. The final result was still similar to the result at room temperature because 0.1 mM sodium citrate is the optimum dosage for the most growth.

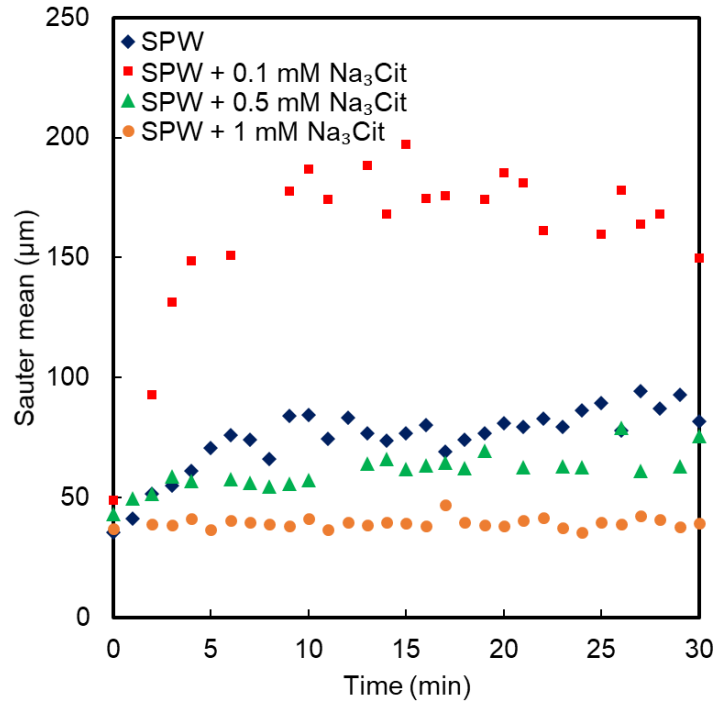


Figure 41. Evolution of Sauter mean bitumen droplet size in synthetic process water at 45°C.

When compared with results at room temperature, it can be seen that the final result at 30 minutes showed a similar trend as at room temperature, but the size grew much faster at the beginning (Figure 42). This means that the effect of sodium citrate is not relative to temperature, but the temperature has a significant influence on coalescence dynamics.

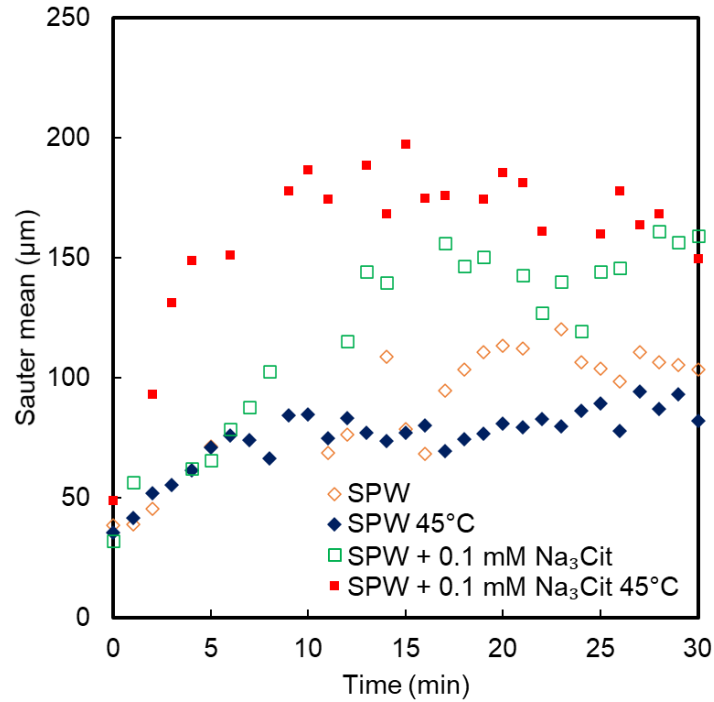


Figure 42. Comparison of the evolution of Sauter mean bitumen droplet size in synthetic process water at room temperature and at 45°C.

5.3. Effect of sodium citrate on surface force between bitumen droplets

Previous zeta potential measurements have shown that the bitumen droplet is more negatively charged with the addition of sodium citrate.^{5,49} For example, bitumen droplet zeta potential is around -40 mV in 1 mM KCl solution. When 0.2 mM sodium citrate was added into the solution, the measured zeta potential became more negative to around -100 mV.⁵

As shown in Figure 43, the sodium citrate effect on zeta potential was similar to previous research. Despite the background calcium ions concentration, the zeta potential of bitumen droplets becomes more negative with increasing sodium citrate concentration. If sodium citrate concentration is lower than calcium ions concentration, the zeta potential

becomes more negative but does not change significantly. However, once sodium citrate concentration is equal to or higher than calcium ions concentration, a more obvious zeta potential change can be seen. For example, with 1 mM calcium ions, the zeta potential only dropped 10 mV from 0 to 0.5 mM sodium citrate addition, but dropped 20 mV from 0.5 to 1 mM sodium citrate addition. In 0.1 mM calcium ions background solution, adding 0.1 mM sodium citrate can readily reduce the zeta potential by 10 mV, and adding 1 mM sodium citrate can reduce the zeta potential by 55 mV.

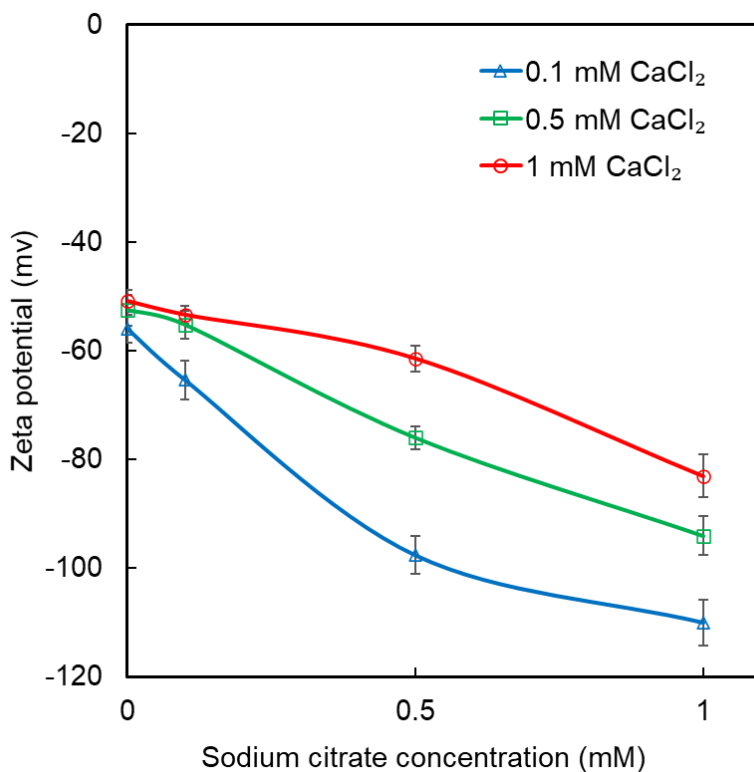


Figure 43. Zeta potential of bitumen droplets in pH 8.5 calcium solution as a function of sodium citrate concentration.

But generally, adding 0.1 mM sodium citrate did not dramatically reduce the zeta potential, especially with higher calcium ions in the background. With 0.5 mM and 1 mM

calcium ions in the background, adding 0.1 mM sodium citrate only changed the zeta potential by 3 mV. This is most likely the reason that 0.1 mM sodium citrate was found to be the optimum dosage for bitumen droplet coalescence.

The same phenomenon happens with sodium citrate in synthetic process water. The zeta potential became more negative with the addition of sodium citrate (Figure 44). The zeta potential decreases by around 15 mV after adding 1 mM sodium citrate.

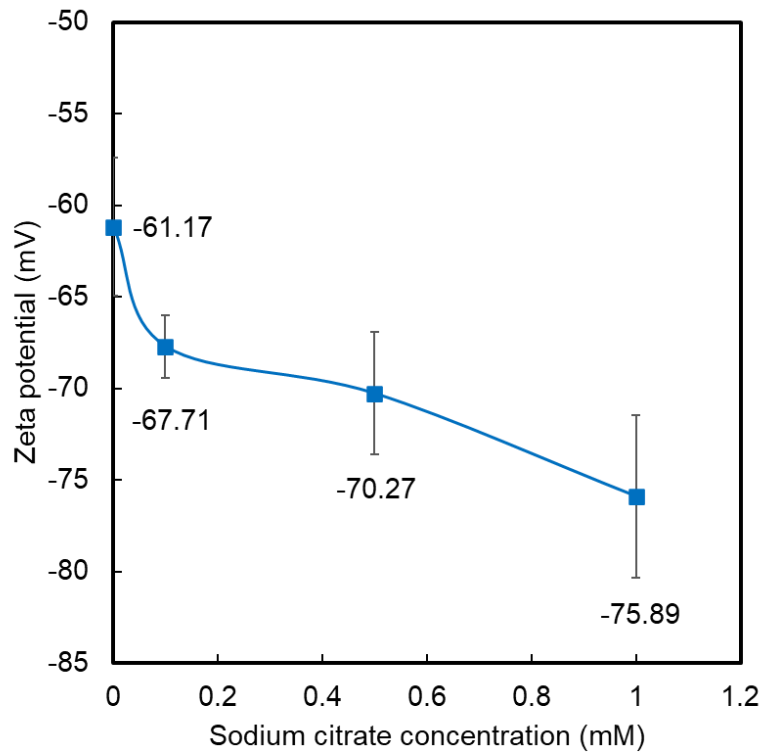


Figure 44. Zeta potential of bitumen droplets in synthetic process water as a function of sodium citrate concentration.

Based on the zeta potential, the colloidal interaction force between two bitumen droplets can be calculated.⁸⁰ The Debye length can be obtained from

$$\kappa^{-1} = \sqrt{\frac{\epsilon\epsilon_0 k_B T}{2 \times 10^3 N_A e^2 C}} \quad (4)$$

where κ^{-1} is the Debye length, C is the ionic strength of the electrolyte in molar units (M or mol/L), ε_0 is the permittivity of free space, ε is the dielectric constant, k_B is the Boltzmann constant, T is the absolute temperature in Kelvin, N_A is the Avogadro number, e is the elementary charge.

EDL and VDW disjoining pressure between two plain surfaces can be calculated by

$$W_{EDL} = \varepsilon\varepsilon_0\kappa \frac{2\psi_1\psi_2e^{-\kappa D} - [\Delta_1\psi_2^2 + \Delta_2\psi_1^2]e^{-2\kappa D}}{1 - \Delta_1\Delta_2e^{-2\kappa D}} \quad (5)$$

$$W_{VDW} = -\frac{A}{12\pi D^3} \quad (6)$$

where W_{EDL} is EDL energy, ψ is the surface charge, D is the distance between two surfaces, Δ is the relative magnitude of the regulation capacitance K_i to the diffuse layer capacitance ($\varepsilon\varepsilon_0\kappa$), which is given by Equation 7

$$\Delta_i = \frac{K_i - \varepsilon\varepsilon_0\kappa}{K_i + \varepsilon\varepsilon_0\kappa} \quad (7)$$

with $-1 \leq \Delta_i \leq 1$. Specifically, the extreme conditions correspond to $\Delta_i = 1$ for the constant surface potential and $\Delta_i = -1$ for the constant surface charge density. In this study, $\Delta_i = 1$ for the constant surface potential.

Based on Derjaguin approximation, the force between two spheres with the same radius is

$$F(D) = 2\pi R(W_{EDL} + W_{VDW}) \quad (8)$$

where F is the surface force, R is the droplet radius.

In this research, surface force is calculated based on the zeta potential from SPW, ionic strength is calculated from the SPW recipe, assuming a droplet radius is 20 μm .

As shown in Figure 45, the interaction force becomes higher with increasing sodium citrate concentration, resulting in a larger energy barrier. With 0.1 mM sodium citrate, the maximum force increases from around 40 nN to 55 nN. While with 1 mM sodium citrate, the force increases from around 40 nN to 75 nN, which almost doubles the force needed for coalescence.

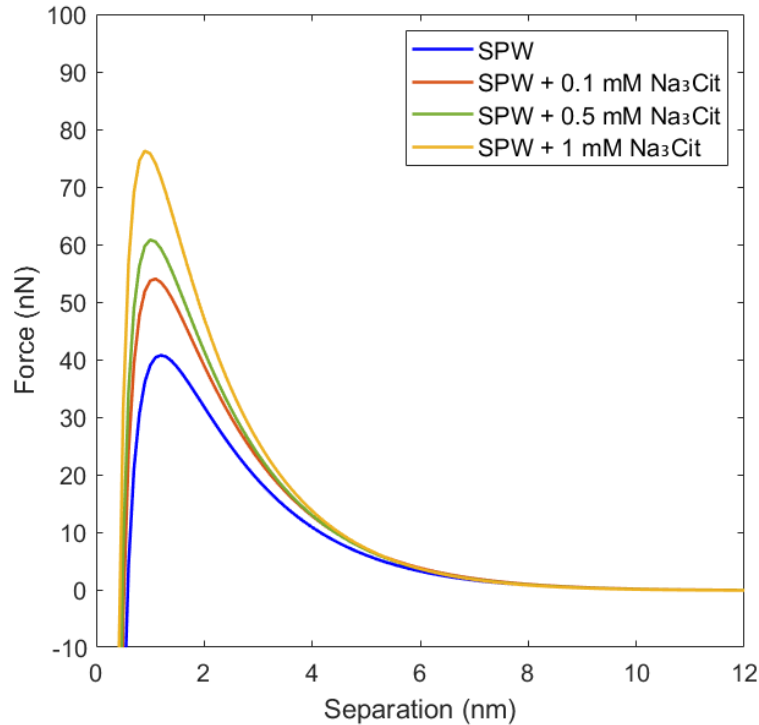


Figure 45. Colloidal interaction force between bitumen droplets in SPW with sodium citrate.

From the results and discussions above, it can be seen that adding sodium citrate would be detrimental to bitumen droplet coalescence based solely on colloidal interactions. With sodium citrate, it takes much more energy for bitumen droplets to overcome the energy barrier and get close enough to coalesce. The increased EDL repulsion is the main reason causing a much higher energy barrier that needs to overcome during the coalescence

process. However, colloidal interaction is not the only factor affecting bitumen droplet coalescence. Bitumen droplet size does not always decrease with increasing sodium citrate concentration. Instead, there is an optimum sodium citrate concentration (0.1 mM in the experiment condition) to achieve the biggest growth.

The overall droplet size growth may depend on the balance of several factors. When sodium citrate concentration is lower, the absolute value of zeta potential increases slightly (less than 10 mV in all experimental sets). The energy barrier could rise by less than 50%, so it may still be possible for bitumen droplets to overcome the energy barrier at this condition. However, the absolute value of the zeta potential increases significantly (could be more than 50 mV) with higher sodium citrate concentration. The energy barrier at this condition could be more than doubled compared to the conditions in the absence of sodium citrate. The droplet size data shows that the size could not grow with 1 mM sodium citrate in SPW, which means that this high energy barrier plays an essential role in inhibiting coalescence.

In conclusion, adding sodium citrate could cause a higher energy barrier for bitumen droplets, which is detrimental to bitumen droplet coalescence. The increase of the energy barrier is much lower if the sodium concentration is low, and bitumen droplets could overcome the energy barrier and coalesce at these conditions. However, if the sodium citrate concentration is high, it could be harder for bitumen droplets to overcome the drastically increased energy barrier, causing a negative impact on coalescence behaviour.

5.4. Effect of sodium citrate on the surface property of bitumen droplets

Asphaltene can form a thin film at the oil-water interface, and the film has been shown to hinder droplet coalescence.⁵⁶⁻⁶⁰ Feng has studied how sodium citrate affects the asphaltene film rheology.⁸¹ When the asphaltene film formed at the oil-water interface, it showed viscous property first, which means the interface is more liquid-like. Asphaltene at the interface then formed a complex structure, showing an elastic property, and the film became more solid-like over time. Ageing time can determine how fast the film property changes. From the preliminary experiment, sodium citrate could increase the ageing time of the asphaltene film, meaning that it may take a longer time for the asphaltene film to become rigid. Sodium citrate also could decrease the yield stress of the film. Therefore, sodium citrate may make the film softer and liquid-like for longer, which may facilitate droplets coalescence. Bitumen film may be similar to asphaltene film at certain conditions, and sodium citrate may also be possible to soften the bitumen film.

5.5. Summary

Sodium citrate as a secondary process aid showed a beneficial effect on the increase of bitumen droplet size at 0.1 mM. However, when sodium citrate was added alone into bitumen emulsion, it did not have any beneficial effect. The negative effect of sodium citrate may be due to the increase of EDL, which increases the electrostatic repulsion between bitumen droplets. At high concentrations, sodium citrate could cause the energy barrier to increase significantly. Consequently, bitumen droplets can barely approach each other and coalesce due to this energy barrier. Besides the negative effect, it is possible that sodium citrate could make the interfacial film between bitumen and water softer. At a lower

concentration, the energy barrier is not too high, and taking into consideration the beneficial effect from the possibly softer film, the overall effect could still be beneficial.

6. Conclusions and future works

6.1. Conclusions

In this study, the effect of sodium citrate on bitumen droplet size has been investigated with different bitumen samples in various water chemistry. Three measuring techniques have been used to show the beneficial effect of sodium citrate on bitumen droplet size growth.

By using a high-speed camera and image analysis technique, bitumen droplet size has been measured with oil sands ores in process water. Caustic has been added in the oil sands extraction process to enhance recovery, showing a significantly beneficial effect on the liberation process. However, caustic had a negative effect on the bitumen droplet coalescence process. With the addition of caustic alone, bitumen droplet size decreased compared to the size in pure process water. Sodium citrate has shown beneficial effects as a secondary process aid for the liberation process as well. In this study, bitumen droplet size increased with the addition of sodium citrate as secondary processing aid.

With SOPAT technology, the evolution of bitumen droplet size was measured in different groups of bitumen-in-process water emulsions. Sodium citrate showed different effects on droplet size depending on the concentration and process water. If sodium citrate was pre-added into process water, a beneficial effect on bitumen droplet size growth at 0.1 mM concentration was observed. However, there was a negative effect of sodium citrate addition at a higher concentration. The same effect was detected in the fines-filtered process water. On the other hand, if sodium citrate was post-added into process water, a negative effect on bitumen droplet coalescence at all tested concentrations was observed.

With SOPAT and FBRM, bitumen droplet size has been measured with bitumen emulsion in synthetic water. With sodium citrate alone in DI water at pH 8.5, there was no significant change in bitumen droplet size, meaning that the addition of sodium citrate individually has no noticeable impact on bitumen droplet size growth. On the other hand, with the presence of calcium ions alone, bitumen droplet size increased with increasing calcium ion concentration. More importantly, if sodium citrate co-existed with calcium ions, there was an optimum sodium citrate concentration to achieve the biggest bitumen droplet size growth. As long as sodium citrate concentration was lower than calcium ions concentration, a positive effect on bitumen droplet coalescence was obtained.

Sodium citrate can affect the bitumen droplet coalescence as a secondary process aid possibly by the interplay of three main factors: slime coating, colloidal interaction, and surface property. The overall balance between these three factors decides whether sodium citrate shows a positive or negative influence on bitumen droplet size.

Sodium citrate could prevent slime coating from happening if added before emulsification⁷⁷. If slime coating had already happened, sodium citrate only had a negative effect on bitumen droplet size growth. If slime coating had been prevented, sodium citrate had a beneficial effect at the optimum dosage. Therefore, the sequence in which sodium citrate was added was a crucial factor. Adding sodium citrate before slime coating happened was the first step to achieve bigger bitumen droplet growth.

Sodium citrate could increase the absolute value of the zeta potential on the bitumen surface, resulting in higher repulsion between droplets. As the concentration of sodium citrate became higher, the energy barrier for bitumen droplets to coalesce increased dramatically. Such a phenomenon makes it almost impossible for bitumen droplets to

aggregate at high sodium citrate concentration (e.g., 1 mM in this study). However, when the sodium citrate concentration was still low (0.1 mM in this study), the energy barrier was relatively low. It could still be possible for two droplets to overcome the energy barrier and other beneficial effects of sodium citrate can still be applied, which could result in a bigger bitumen droplet size.

Sodium citrate may change the surface properties of bitumen droplets, possibly interfacial film softness. The softer interfacial film might enhance the coalescence of bitumen droplet.

In conclusion, sodium citrate had a significant beneficial effect on bitumen droplet size growth if added as a secondary process aid, but did not have a beneficial effect on bitumen droplet size growth individually. The effects of sodium citrate depend on the balance of three factors: slime coating, colloidal interaction and surface property.

6.2. Future works

1) The bitumen droplet coalescence process in the real system also involves hydrodynamic interactions. In this study, the hydrodynamic condition has been kept the same to compare each experiment in sets of experiments. However, shear could play a crucial role in the bitumen droplet coalescence process. Studies have been done with the micropipette technique to show the coalescence probability with different shear conditions and water chemistry.^{38,39,82} It would be more comprehensive to confirm the results with micropipette at different shear conditions. With higher shear and softer bitumen film caused by sodium citrate, the beneficial effect of sodium citrate may be more obvious.

2) In this study, the colloidal interaction was calculated based on the measured zeta potential. In order to understand if sodium citrate also affects other forces, such as steric hindrance, force measurement by atomic force measurement (AFM) or other equipment is needed.

3) The bitumen droplet coalescence process contains 3 sub-steps: thin film formation, film drainage, and film rupture. The softer film caused by sodium citrate may be beneficial for film rupture, but the detailed mechanism and its effect on film drainage are still unknown. Using a technique such as the dynamic force apparatus (DFA) may be helpful to understand this mechanism.

References

- (1) Government of Canada. Crude oil facts <https://www.nrcan.gc.ca/science-data/data-analysis/energy-data-analysis/energy-facts/crude-oil-facts/20064>.
- (2) Masliyah, J. H.; Czarnecki, J.; Xu, Z. *Handbook on Theory and Practice of Bitumen Recovery from Athabasca Oil Sands*; 2011; Vol. 1. <https://doi.org/10.1017/CBO9781107415324.004>.
- (3) Long, J.; Gu, Y. J. Sodium Citrate and Caustic as Process Aids for the Extraction of Bitumen from Mined Oil Sands. US9469814B2, January 28, 2015.
- (4) Long, J. Optimized Caustic Control Based on Ore Grade and Fines Content for Bitumen Extraction from Mined Oil Sands. US9458386B2, October 4, 2016.
- (5) Xiang, B.; Truong, N. T. V.; Feng, L.; Bai, T.; Qi, C.; Liu, Q. Study of the Role of Sodium Citrate in Bitumen Liberation. *Energy & Fuels* **2019**, *33* (9), 8271–8278. <https://doi.org/10.1021/acs.energyfuels.9b01788>.
- (6) Xiang, B.; Liu, Q.; Long, J. Probing Bitumen Liberation by a Quartz Crystal Microbalance with Dissipation. *Energy and Fuels* **2018**, *32* (7), 7451–7457. <https://doi.org/10.1021/acs.energyfuels.8b01285>.
- (7) Sanford, E. C. Processibility of Athabasca Oil Sand: Interrelationship between Oil Sand Fine Solids, Process Aids, Mechanical Energy and Oil Sand Age after Mining. *The Canadian Journal of Chemical Engineering* **1983**, *61* (4), 554–567. <https://doi.org/10.1002/cjce.5450610410>.
- (8) Wallace, D.; Henry, D.; Takamura, K. A Physical Chemical Explanation for Deterioration in the Hot Water Processability of Athabasca Oil Sand Due to Aging.

- Fuel Science and Technology International* **1989**, 7 (5–6), 699–725.
<https://doi.org/10.1080/08843758908962265>.
- (9) Masliyah, J.; Zhou, Z. J.; Xu, Z.; Czarnecki, J.; Hamza, H. Understanding Water-Based Bitumen Extraction from Athabasca Oil Sands. *The Canadian Journal of Chemical Engineering* **2008**, 82 (4), 628–654.
<https://doi.org/10.1002/cjce.5450820403>.
- (10) Liu, J.; Xu, Z.; Masliyah, J. Colloidal Forces between Bitumen Surfaces in Aqueous Solutions Measured with Atomic Force Microscope. *Colloids and Surfaces A: Physicochemical and Engineering Aspects* **2005**, 260 (1–3), 217–228.
<https://doi.org/10.1016/j.colsurfa.2005.03.026>.
- (11) Clark, K. A. Hot Water Separation of Alberta Bituminous Sand. *Trans. Can. Inst. Min. Metall* **1944**, 47, 257–274.
- (12) Clark, K. A. Athabasca Oil Sands—Fundamentals Affecting Development. *Can. Pet* **1966**, 7, 18–21.
- (13) Basu, S.; Nandakumar, K.; Masliyah, J. H. On Bitumen Liberation from Oil Sands. *The Canadian Journal of Chemical Engineering* **1997**, 75 (2), 476–479.
<https://doi.org/10.1002/cjce.5450750224>.
- (14) Basu, S.; Nandakumar, K.; Masliyah, J. H. Effect of NaCl and MIBC/Kerosene on Bitumen Displacement by Water on a Glass Surface. *Colloids and Surfaces A: Physicochemical and Engineering Aspects* **1998**, 136 (1–2), 71–80.
[https://doi.org/10.1016/S0927-7757\(97\)00251-3](https://doi.org/10.1016/S0927-7757(97)00251-3).

- (15) Zhao, H.; Long, J.; Masliyah, J. H.; Xu, Z. Effect of Divalent Cations and Surfactants on Silica-Bitumen Interactions. *Industrial and Engineering Chemistry Research* **2006**, *45* (22), 7482–7490. <https://doi.org/10.1021/ie060348o>.
- (16) Liu, J.; Xu, Z.; Masliyah, J. Studies on Bitumen-Silica Interaction in Aqueous Solutions by Atomic Force Microscopy. *Langmuir* **2003**, *19* (9), 3911–3920. <https://doi.org/10.1021/la0268092>.
- (17) Srinivasa, S.; Flury, C.; Afacan, A.; Masliyah, J.; Xu, Z. Study of Bitumen Liberation from Oil Sands Ores by Online Visualization. *Energy and Fuels* **2012**, *26* (5), 2883–2890. <https://doi.org/10.1021/ef300170m>.
- (18) Moran, K.; Masliyah, J.; Yeung, A. Factors Affecting the Aeration of Small Bitumen Droplets. *Canadian Journal of Chemical Engineering* **2000**, *78* (4), 625–634. <https://doi.org/10.1002/cjce.5450780404>.
- (19) Najafi, A. S.; Xu, Z.; Masliyah, J. Measurement of Sliding Velocity and Induction Time of a Single Micro-Bubble under an Inclined Collector Surface. *The Canadian Journal of Chemical Engineering* **2008**, *86* (6), 1001–1010. <https://doi.org/10.1002/cjce.20116>.
- (20) Gu, G.; Xu, Z.; Nandakumar, K.; Masliyah, J. Effects of Physical Environment on Induction Time of Air-Bitumen Attachment. *International Journal of Mineral Processing* **2003**, *69* (1–4), 235–250. [https://doi.org/10.1016/S0301-7516\(02\)00128-X](https://doi.org/10.1016/S0301-7516(02)00128-X).
- (21) Boxall, J. A.; Koh, C. A.; Sloan, E. D.; Sum, A. K.; Wu, D. T. Measurement and Calibration of Droplet Size Distributions in Water-in-Oil Emulsions by Particle Video Microscope and a Focused Beam Reflectance Method. *Industrial and*

- Engineering Chemistry Research* **2010**, *49* (3), 1412–1418.
<https://doi.org/10.1021/ie901228e>.
- (22) Podgorski, D. C.; Corilo, Y. E.; Nyadong, L.; Lobodin, V. v.; Bythell, B. J.; Robbins, W. K.; McKenna, A. M.; Marshall, A. G.; Rodgers, R. P. Heavy Petroleum Composition. 5. Compositional and Structural Continuum of Petroleum Revealed. *Energy & Fuels* **2013**, *27* (3), 1268–1276. <https://doi.org/10.1021/ef301737f>.
- (23) Derjaguin, B.; Landau, L. Theory of the Stability of Strongly Charged Lyophobic Sols and of the Adhesion of Strongly Charged Particles in Solutions of Electrolytes. *Acta Physicochim. URSS* **1941**, *14* (633).
- (24) Verwey, E. J. W. Theory of the Stability of Lyophobic Colloids. *Journal of Physical and Colloid Chemistry* **1947**, *51* (3), 631–636.
<https://doi.org/10.1021/j150453a001>.
- (25) Wu, X.; Czarnecki, J.; Hamza, N.; Masliyah, J. Interaction Forces between Bitumen Droplets in Water. *Langmuir* **1999**, *15* (16), 5244–5250.
<https://doi.org/10.1021/la981546q>.
- (26) Healy, T. W.; White, L. R. Ionizable Surface Group Models of Aqueous Interfaces. *Advances in Colloid and Interface Science* **1978**, *9* (4), 303–345.
[https://doi.org/10.1016/0001-8686\(78\)85002-7](https://doi.org/10.1016/0001-8686(78)85002-7).
- (27) Levine, S.; Smith, A. L. Theory of the Differential Capacity of the Oxide/Aqueous Electrolyte Interface. *Discussions of the Faraday Society* **1971**, *52*, 290–301.
<https://doi.org/10.1039/DF9715200290>.

- (28) Takamura, K.; Chow, R. S. The Electric Properties of the Bitumen/Water Interface Part II. Application of the Ionizable Surface-Group Model. *Colloids and Surfaces* **1985**, *15* (C), 35–48. [https://doi.org/10.1016/0166-6622\(85\)80053-6](https://doi.org/10.1016/0166-6622(85)80053-6).
- (29) Dezhi, S.; Shik Chung, J.; Xiaodong, D.; Ding, Z. Demulsification of Water-in-Oil Emulsion by Wetting Coalescence Materials in Stirred- and Packed-Columns. *Colloids and Surfaces A: Physicochemical and Engineering Aspects* **1999**, *150* (1–3), 69–75. [https://doi.org/10.1016/S0927-7757\(98\)00590-1](https://doi.org/10.1016/S0927-7757(98)00590-1).
- (30) Eow, J. S.; Ghadiri, M.; Sharif, A. O.; Williams, T. J. Electrostatic Enhancement of Coalescence of Water Droplets in Oil: A Review of the Current Understanding. *Chemical Engineering Journal* **2001**, *84* (3), 173–192. [https://doi.org/10.1016/S1385-8947\(00\)00386-7](https://doi.org/10.1016/S1385-8947(00)00386-7).
- (31) Gochev, G. Thin Liquid Films Stabilized by Polymers and Polymer/Surfactant Mixtures. *Current Opinion in Colloid & Interface Science* **2015**, *20* (2), 115–123. <https://doi.org/10.1016/J.COCIS.2015.03.003>.
- (32) Rommel, W.; Meon, W.; Blass, E. Hydrodynamic Modeling of Droplet Coalescence at Liquid-Liquid Interfaces. *Separation Science and Technology* **1992**, *27* (2), 129–159. <https://doi.org/10.1080/01496399208018870>.
- (33) Klaseboer, E.; Chevaillier, J. P.; Gourdon, C.; Masbernat, O. Film Drainage between Colliding Drops at Constant Approach Velocity: Experiments and Modeling. *Journal of Colloid and Interface Science* **2000**, *229* (1), 274–285. <https://doi.org/10.1006/jcis.2000.6987>.

- (34) Charles, G. E.; Mason, S. G. The Coalescence of Liquid Drops with Flat Liquid/Liquid Interfaces. *Journal of Colloid Science* **1960**, *15* (3), 236–267. [https://doi.org/10.1016/0095-8522\(60\)90026-X](https://doi.org/10.1016/0095-8522(60)90026-X).
- (35) Mohammed, R. A.; Bailey, A. I.; Luckham, P. F.; Taylor, S. E. Dewatering of Crude Oil Emulsions 2. Interfacial Properties of the Asphaltic Constituents of Crude Oil. *Colloids and Surfaces A: Physicochemical and Engineering Aspects* **1993**, *80* (2–3), 237–242. [https://doi.org/10.1016/0927-7757\(93\)80203-Q](https://doi.org/10.1016/0927-7757(93)80203-Q).
- (36) Laroche, I. Investigating the Stability of Bitumen Droplets in Water through Force Measurements, Edmonton, 2000. <https://doi.org/10.7939/R3707WS6N>.
- (37) Aksoy, B. S. Hydrophobic Forces in Free Thin Films of Water in the Presence and Absence of Surfactants, Virginia Tech, Blacksburg, 1997.
- (38) Yeung, A.; Moran, K.; Masliyah, J.; Czarnecki, J. Shear-Induced Coalescence of Emulsified Oil Drops. *Journal of Colloid and Interface Science* **2003**, *265* (2), 439–443. [https://doi.org/10.1016/S0021-9797\(03\)00531-9](https://doi.org/10.1016/S0021-9797(03)00531-9).
- (39) Lin, F. Surface Charge Heterogeneities and Shear-Induced Coalescence of Bitumen Droplets, Edmonton, 2012. <https://doi.org/10.7939/R3N59W>.
- (40) Esmaili, P.; Lin, F.; Yeung, A. Stability of Emulsified Heavy Oil: The Combined Effects of Deterministic DLVO Forces and Random Surface Charges. *Langmuir* **2012**, *28* (11), 4948–4954. <https://doi.org/10.1021/la204254m>.
- (41) Stancik, E. J.; Kouhkan, M.; Fuller, G. G. Coalescence of Particle-Laden Fluid Interfaces. *Langmuir* **2004**, *20* (1), 90–94. <https://doi.org/10.1021/la0356093>.

- (42) Whitby, C. P.; Fischer, F. E.; Fornasiero, D.; Ralston, J. Shear-Induced Coalescence of Oil-in-Water Pickering Emulsions. *Journal of Colloid and Interface Science* **2011**, *361* (1), 170–177. <https://doi.org/10.1016/j.jcis.2011.05.046>.
- (43) Rogel, E. Asphaltene Aggregation: A Molecular Thermodynamic Approach. *Langmuir* **2002**, *18* (5), 1928–1937. <https://doi.org/10.1021/la0109415>.
- (44) Natarajan, A.; Xie, J.; Wang, S.; Masliyah, J.; Zeng, H.; Xu, Z. Understanding Molecular Interactions of Asphaltenes in Organic Solvents Using a Surface Force Apparatus. *Journal of Physical Chemistry C* **2011**, *115* (32), 16043–16051. <https://doi.org/10.1021/jp2039674>.
- (45) Wang, S.; Liu, J.; Zhang, L.; Xu, Z.; Masliyah, J. Colloidal Interactions between Asphaltene Surfaces in Toluene. *Energy and Fuels* **2009**, *23* (2), 862–869. <https://doi.org/10.1021/ef800812k>.
- (46) Yoon, R. H.; Guzonas, D.; Aksoy, B.; Czarnecki, J. Role of Surface Forces in Tar Sand Processing; Vancouver, 1995.
- (47) Yoon, R. H.; Rabinovich, Y. Role of Asphaltene in the Processing of Tar Sand, Polymers in Mineral Processing; Vancouver, 1999.
- (48) Moschopedis, S. E.; Fryer, J. F.; Speight, J. G. Water-Soluble Constituents of Athabasca Bitumen. *Fuel*. 1977, pp 109–110. [https://doi.org/10.1016/0016-2361\(77\)90053-9](https://doi.org/10.1016/0016-2361(77)90053-9).
- (49) Gan, W.; Liu, Q. Coagulation of Bitumen with Kaolinite in Aqueous Solutions Containing Ca^{2+} , Mg^{2+} and Fe^{3+} : Effect of Citric Acid. *Journal of Colloid and Interface Science* **2008**, *324* (1–2), 85–91. <https://doi.org/10.1016/j.jcis.2008.05.009>.

- (50) Langevin, D.; Argillier, J.-F. Interfacial Behavior of Asphaltenes. *Advances in Colloid and Interface Science* **2016**, *233*, 83–93. <https://doi.org/10.1016/j.cis.2015.10.005>.
- (51) Alvarez-Ramírez, F.; Ruiz-Morales, Y. Island versus Archipelago Architecture for Asphaltenes: Polycyclic Aromatic Hydrocarbon Dimer Theoretical Studies. *Energy and Fuels* **2013**, *27* (4), 1791–1808. <https://doi.org/10.1021/ef301522m>.
- (52) Chilingarian, G. V. *Bitumens, Asphalts, and Tar Sands*; Elsevier, 2011.
- (53) Mullins, O. C. The Modified Yen Model. *Energy and Fuels* **2010**, *24* (4), 2179–2207. <https://doi.org/10.1021/ef900975e>.
- (54) Mullins, O. C.; Sabbah, H.; Eyssautier, J.; Pomerantz, A. E.; Barré, L.; Andrews, A. B.; Ruiz-Morales, Y.; Mostowfi, F.; McFarlane, R.; Goual, L.; Lepkowicz, R.; Cooper, T.; Orbulescu, J.; Leblanc, R. M.; Edwards, J.; Zare, R. N. Advances in Asphaltene Science and the Yen-Mullins Model. *Energy and Fuels* **2012**, *26* (7), 3986–4003. <https://doi.org/10.1021/ef300185p>.
- (55) Mullins, O. C. The Asphaltenes. *Annual Review of Analytical Chemistry* **2011**, *4* (1), 393–418. <https://doi.org/10.1146/annurev-anchem-061010-113849>.
- (56) Li, M.; Xu, M.; Ma, Y.; Wu, Z.; Christy, A. A. Interfacial Film Properties of Asphaltenes and Resins. *Fuel* **2002**, *81* (14), 1847–1853. [https://doi.org/10.1016/S0016-2361\(02\)00050-9](https://doi.org/10.1016/S0016-2361(02)00050-9).
- (57) Yarranton, H. W.; Hussein, H.; Masliyah, J. H. Water-in-Hydrocarbon Emulsions Stabilized by Asphaltenes at Low Concentrations. *Journal of colloid and interface science* **2000**, *228* (1), 52–63.

- (58) Ortiz, D. P.; Baydak, E. N.; Yarranton, H. W. Effect of Surfactants on Interfacial Films and Stability of Water-in-Oil Emulsions Stabilized by Asphaltenes. *Journal of Colloid and Interface Science* **2010**, *351* (2), 542–555. <https://doi.org/https://doi.org/10.1016/j.jcis.2010.08.032>.
- (59) Tchoukov, P.; Czarnecki, J.; Dabros, T. Study of Water-in-Oil Thin Liquid Films: Implications for the Stability of Petroleum Emulsions. *Colloids and Surfaces A: Physicochemical and Engineering Aspects* **2010**, *372* (1–3), 15–21. <https://doi.org/10.1016/j.colsurfa.2010.09.007>.
- (60) Khristov, K.; Taylor, S. D.; Czarnecki, J.; Masliyah, J. Thin Liquid Film Technique - Application to Water-Oil-Water Bitumen Emulsion Films. *Colloids and Surfaces A: Physicochemical and Engineering Aspects* **2000**, *174* (1–2), 183–196. [https://doi.org/10.1016/S0927-7757\(00\)00510-0](https://doi.org/10.1016/S0927-7757(00)00510-0).
- (61) Tchoukov, P.; Yang, F.; Xu, Z.; Dabros, T.; Czarnecki, J.; Sjöblom, J. Role of Asphaltenes in Stabilizing Thin Liquid Emulsion Films. *Langmuir* **2014**, *30* (11), 3024–3033. <https://doi.org/10.1021/la404825g>.
- (62) Liu, J.; Zhang, L.; Xu, Z.; Masliyah, J. Colloidal Interactions between Asphaltene Surfaces in Aqueous Solutions. *Langmuir* **2006**, *22* (4), 1485–1492. <https://doi.org/10.1021/la052755v>.
- (63) Shi, C.; Zhang, L.; Xie, L.; Lu, X.; Liu, Q.; Mantilla, C. A.; van den Berg, F. G. A.; Zeng, H. Interaction Mechanism of Oil-in-Water Emulsions with Asphaltenes Determined Using Droplet Probe AFM. *Langmuir* **2016**, *32* (10), 2302–2310. <https://doi.org/10.1021/acs.langmuir.5b04392>.

- (64) Liu, J.; Xu, Z.; Masliyah, J. Role of Fine Clays in Bitumen Extraction from Oil Sands. *AIChE Journal* **2004**, *50* (8), 1917–1927. <https://doi.org/10.1002/aic.10174>.
- (65) Liu, J.; Xu, Z.; Masliyah, J. Interaction between Bitumen and Fines in Oil Sands Extraction System: Implication to Bitumen Recovery. *Canadian Journal of Chemical Engineering* **2004**, *82* (4), 655–666. <https://doi.org/10.1002/cjce.5450820404>.
- (66) Bakhtiari, M. T.; Harbottle, D.; Curran, M.; Ng, S.; Spence, J.; Siy, R.; Liu, Q.; Masliyah, J.; Xu, Z. Role of Caustic Addition in Bitumen-Clay Interactions. *ACS Publications* **2015**, *29* (1), 58–69. <https://doi.org/10.1021/ef502088z>.
- (67) Liu, J.; Zhou, Z.; Xu, Z.; Masliyah, J. Bitumen–Clay Interactions in Aqueous Media Studied by Zeta Potential Distribution Measurement. *Journal of Colloid and Interface Science* **2002**, *252* (2), 409–418. <https://doi.org/10.1006/jcis.2002.8471>.
- (68) Hannisdal, A.; Ese, M. H.; Hemmingsen, P. v.; Sjöblom, J. Particle-Stabilized Emulsions: Effect of Heavy Crude Oil Components Pre-Adsorbed onto Stabilizing Solids. *Colloids and Surfaces A: Physicochemical and Engineering Aspects* **2006**, *276* (1–3), 45–58. <https://doi.org/10.1016/j.colsurfa.2005.10.011>.
- (69) Li, A. Role of Clays in Bitumen Extraction of Water-Based Oil Sands Processing, Edmonton, 2019. <https://doi.org/10.7939/R3-8SAA-8952>.
- (70) Nallamilli, T.; Basavaraj, M. G. Synergistic Stabilization of Pickering Emulsions by in Situ Modification of Kaolinite with Non Ionic Surfactant. *Applied Clay Science* **2017**, *148*, 68–76. <https://doi.org/10.1016/j.clay.2017.07.038>.

- (71) Whitby, C. P.; Fornasiero, D.; Ralston, J. Structure of Oil-in-Water Emulsions Stabilised by Silica and Hydrophobised Titania Particles. *Journal of Colloid and Interface Science* **2010**, *342* (1), 205–209. <https://doi.org/10.1016/j.jcis.2009.10.068>.
- (72) Dongbao, F.; Woods, J. R.; Kung, J.; Kingston, D. M.; Kotlyar, L. S.; Sparks, B. D.; Mercier, P. H. J.; McCracken, T.; Ng, S. Residual Organic Matter Associated with Toluene-Extracted Oil Sands Solids and Its Potential Role in Bitumen Recovery via Adsorption onto Clay Minerals. *Energy and Fuels* **2010**, *24* (4), 2249–2256. <https://doi.org/10.1021/ef900885p>.
- (73) Chen, Z.; Li, Z. Preparation and Stabilisation Mechanism of Asphalt-in-Water Pickering Emulsion Stabilised by SiO₂ Nanoparticles. *Road Materials and Pavement Design* **2020**, 1–13. <https://doi.org/10.1080/14680629.2019.1708431>.
- (74) Li, C.; Li, J.; Hu, Y. Research on Physics Stability of Emulsified Asphalt Modified by Nano Silica. *IOP Conference Series: Materials Science and Engineering* **2019**, *562*, 012003. <https://doi.org/10.1088/1757-899x/562/1/012003>.
- (75) Gupta, M. *Practical Guide to Vegetable Oil Processing*; 2017.
- (76) Bai, T.; Grundy, J. S.; Manica, R.; Li, M.; Liu, Q. Controlling the Interaction Forces between an Air Bubble and Oil with Divalent Cations and Sodium Citrate. *Journal of Physical Chemistry C* **2020**, *124* (32), 17622–17631. <https://doi.org/10.1021/acs.jpcc.0c04108>.
- (77) Zhang, D. Effects of Sodium Citrate on Slime Coatings in Bitumen Extraction, Edmonton, 2020. <https://doi.org/10.7939/R3-DX6H-8239>.
- (78) Zhao, H.; Dang-Vu, T.; Long, J.; Xu, Z.; Masliyah, J. H. Role of Bicarbonate Ions in Oil Sands Extraction Systems with a Poor Processing Ore. *Journal of Dispersion*

Science and Technology **2009**, *30* (6), 809–822.
<https://doi.org/10.1080/01932690802643980>.

- (79) Schümann, H.; Khatibi, M.; Tutkun, M.; H. Pettersen, B.; Yang, Z.; Nydal, O. J. Droplet Size Measurements in Oil–Water Dispersions: A Comparison Study Using FBRM and PVM. *Journal of Dispersion Science and Technology* **2015**, *36* (10), 1432–1443. <https://doi.org/10.1080/01932691.2014.989569>.
- (80) Carnie, S. L.; Chan, D. Y. C. Interaction Free Energy between Plates with Charge Regulation: A Linearized Model. *Journal of Colloid and Interface Science* **1993**, *161* (1), 260–264. <https://doi.org/10.1006/jcis.1993.1464>.
- (81) Feng, L. *Effect of Sodium Citrate on Asphaltene Film at Oil-Water Interface*; Edmonton, 2021.
- (82) Yeung, A.; Dabros, T.; Masliyah, J.; Czarnecki, J. Micropipette: A New Technique in Emulsion Research. *Colloids and Surfaces A: Physicochemical and Engineering Aspects* **2000**. [https://doi.org/10.1016/S0927-7757\(00\)00509-4](https://doi.org/10.1016/S0927-7757(00)00509-4).